Doctoral Dissertation

Development of Generalized Multimedia Model for Analyzing Harmful Environmental Chemicals

（環境中有害物質評価のための汎用型マルチメディアモデルの開発）

Shengyun Li

December 2023

Graduate School of Engineering,

Osaka University

Preface

The dissertation entitled “The development of generalized multimedia model for analyzing harmful environmental chemicals” is submitted for the degree of Doctor of Engineering at Osaka University in Japan. The study described herein was conducted under the supervision of Professor Akira Kondo, Ph.D. and Associate Professor Hikari Shimadera, Ph.D., and Assistant Professor Tomohito Matsuo, Ph.D. in the Laboratory of Engineering for Assessing the Sustainable Environment, Division of Sustainable Energy and Environmental Engineering, Graduate school of Engineering during the period of April 2019 to March 2024.

This study integrates and upgrades previous research. The author hope that this study will attract scholars' interest in environmental modeling and environmental management organizations can conduct more efficient management and formulate more scientific policies.

Shengyun Li

Ph.D. student

Graduate School of Engineering

Osaka University

Acknowledgement

The author received a great deal of care and practical assistance while completing the doctoral program and writing this dissertation. The author's research began at the master's degree and has benefited from the assistance of numerous individuals.

First and foremost, I wish to express my heartfelt gratitude to Professor Akira Kondo, my dissertation supervisor. On my journey of scientific research, he was my guiding mentor. During my early exploration of environmental studies, it was he who introduced me to environmental modeling, solidified my desire to pursue a doctoral degree, and accepted me as his student. Over these years, he has provided me with countless invaluable advice and guidance and kindness that words fail to express. I also express gratitude to him for providing me with the opportunity to study and live in Osaka University, Japan.

Second, I would like to express my heartfelt gratitude to Associate Professor Hikari Shimadera, who assisted me in every detail of all the studies. I am deeply impressed by his expertise and technical prowess. He has imparted to me a wealth of knowledge in various environmental models and programming skills, enabling me to efficiently pursue results in my research.

I am also very grateful to Assistant Professor Tomohito Matsuo for his supports throughout my research. He has provided me with significant assistance in the writing of my dissertation and the publication of academic articles.

Additionally, I'd like to thank all the members of the Laboratory of Engineering for Assessing the Sustainable Environment for their unwavering support of my research and personal life. As a foreigner, without their assistance, I would have struggled to navigate campus life and complete my research with peace of mind.

Finally, the author would like to express my gratitude to my family and friends for their support and encouragement throughout the years of study.

Abstract

Along with the intensification of human industrial production, the resulting environmental pollution problems have brought various kinds of troubles to people. When environmental pollution occurs, it requires financial and human resources to remedy the situation. Although current environmental technology can significantly reduce the harm caused by pollutions, it is wiser to prevent and manage the pollution in advance. Governments and public authorities are responsible for environmental monitoring and management.

Currently, the main method of environmental monitoring is the deployment of monitoring stations in cities, especially the urban area. Data are measured automatically or manually at regular intervals by instruments and submitted to regulatory agencies. Even if these methods have been utilized, monitoring environment in a large geographical region (such as the whole nation or local prefecture) in real time is not possible. It is feasible to monitor such as air quality in urban centers in real time using automated detection equipment, but deploying such high-technology equipment would be significant expensive. In addition, there are some areas where it is difficult to deploy fixed monitoring equipment, such as water bodies, and manual labor (environmental inspectors) would have to be dispatched for sampling and chemical analysis. Moreover, the deployment of monitoring sites is critical. Since most of the detection sites are deployed in city centers, errors will inevitably occur if their detection results are regarded as the environmental state of the entire city. To improve the accuracy of monitoring, the number of detection sites must be increased and deployed as evenly as possible throughout the region. However, it is impractical to deploy such a dense number of environmental monitoring stations.

Considering the practical difficulty in monitoring and the adverse health effects of harmful environmental pollutions, it is important to evaluate the environment in another way. Mathematical models have been developed as an approach to evaluate our environment. Various studies ranging from modeling macro-scale environmental issues to localized micro-scale environmental assessments can be found in research papers.

We can now predict the concentration of environmental chemical pollutions using different mathematical models. However, these environmental models have their limitations. In most models, the study area was treated as a homogeneous area and the concentration of pollutant was not distributed in space. Also, the emission of pollutant was homogeneous in whole area, these models only use the total emission as the input data. These simplifications and assumptions reduce the accuracy of model results and amplify the uncertainty of subsequent studies based on these data.

To solve these problems, a generalized distributed multimedia environment model was developed in this study. This model divides the real space into four environmental media: atmosphere, water, soil, and sediment. The model considers mass balance by summing all mass transfers between the environmental media: equilibrium, emission, advection, deposition and sedimentation. In addition, this model makes a high-resolution division of the target area, considering the dynamic balance of the environment within the basic unit and the mutual influence between the units. The calculus idea is adopted to represent the real environmental situation of the location with the calculation results of the subdivided units.

In this study, the model was applied to three different types of pollutants and simulations were performed in the Lake Biwa and Yodo River basin in Japan. The pollutant emissions in the target area were estimated. Meteorological and hydrological data were also integrated as inputs. The model was calculated for different types of pollutants to simulate the concentrations over the past decades. The feasibility and accuracy of the model were evaluated by comparing the measured values with the calculated results of the model. The averaged calculation results showed that the model can simulate and reproduce past observations well. By comparing the data from the sampled basic units with the data from the real observatories, it was found that the model could reflect the distribution of pollutants in a specific area.

The modeling and problem-solving methodology of this study provides a novel way of thinking about environmental testing. The model is scalable and can be applied to

other regions and to other types of pollutants by modifying the parameters and equations of the model.

Index

1 Introduction

1.1 Background

Environmental pollution caused by human production activities has become an increasingly serious problem since the Industrial Revolution. Hazardous chemicals such as heavy metals, Pharmaceuticals and Personal Care Products (PPCPs) and Volatile organic compounds (VOCs) have been emitted to environment for decades via human industrial activities. Many of the PPCPs were already detected in groundwater (Xu et al., 2019; Ma et al., 2022) and basin (Singh and Suthar, 2021). Beside occurred in the surface water (Li et al., 2021) and sediment (Abdel Gawad, 2018; Gholizadeh and Patimar, 2018), heavy metals were also detected in urban mangroves (Chai et al., 2019). Heavy metals were commonly detected in water, in soil and in sediment (Schipper et al., 2011; Ali and Khan, 2018; Alghamdi et al., 2019).

These hazardous chemicals may damage health and ecosystems. For instance, VOCs could cause detrimental effects on human health and shows high toxicities (Kampa and Castanas, 2008; Ramírez et al., 2012; Li et al., 2013). PPCPs also show health risk and ecotoxicity in different environmental media (Boxall et al., 2012; Liu et al., 2019a). Human body can absorb heavy metals by different way. Typical toxic heavy metals in the environment (such as As, Cd, Cr, Hg and Pb) can be taken in through the food chain (Douay et al., 2013; Yu et al., 2020). Heavy metals can cause severe damage and toxic effects to fishes (Raknuzzaman et al., 2016; Gu et al., 2017) and crops (Abou-Elwafa et al., 2019) which may damage the ecosystem. Heavy metals can affected marine life (Raknuzzaman et al., 2016; Gu et al., 2017) and terrestrial plants (Douay et al., 2013; Abou-Elwafa et al., 2019). For instance, heavy metals were absorbed in drinking water (Chowdhury et al., 2016), edible animals (Krasnići et al., 2013; Karar et al., 2019; Wang et al., 2021), vegetables (Liu et al., 2021), fruits and their secondary products (Orescanin et al., 2003; Prabagar et al., 2021). More relevant to human life, heavy metals even already detected in populated city (Liang et al., 2015; Singh and Suthar, 2021; Peng et al., 2022) which may damage citizens' health. Heavy metals could cause

DNA damage (Boxall et al., 2012), increase the chance of antibiotic resistance (Yang et al., 2017) and are associated with an increased risk of cardiovascular, kidney (Lentini et al., 2009; Buhari et al., 2019). Thus, as important as pollution treatment, these components are requested under longtime monitoring and risk assessment due to their identified ecotoxicity and health toxicity.

Currently, the main method of environmental monitoring is the deployment of monitoring stations in cities, especially the urban area. Data are measured automatically or manually at regular intervals by instruments and submitted to regulatory agencies. Even if these methods have been utilized, monitoring environment in a large geographical region (such as the whole nation or local prefecture) in real time is not possible. It is feasible to monitor such as air quality in urban centers in real time using automated detection equipment, but deploying such high-technology equipment would be significant expensive. In addition, there are some areas where it is difficult to deploy fixed monitoring equipment, such as water bodies, and manual labor (environmental inspectors) would have to be dispatched for sampling and chemical analysis. Moreover, the deployment of monitoring sites is critical. Since most of the detection sites are deployed in city centers, errors will inevitably occur if their detection results are regarded as the environmental state of the entire city. To improve the accuracy of monitoring, the number of detection sites must be increased and deployed as evenly as possible throughout the region. However, it is impractical to deploy such a dense number of environmental monitoring stations. Considering the practical difficulty in monitoring and the adverse health effects of harmful environmental pollutions, it is important to evaluate the environment in another way.

1.2 Previous study

Mathematical models have been developed as an approach to evaluate our environment. Various mathematical models have been developed and utilized to different environmental pollutants including organic components and heavy metals. For instance, Level III multimedia model which based on fugacity was developed and applied to organic chemicals by Mackay et al. (1985) and Mackay and Paterson (1991). Various

organic chemicals were estimate fate, transport, and steady state concentrations in the environment using Level III fugacity model (Edwards et al., 1999). In order to simulate and predict the fate of heavy metals in lakes and rivers, QWASI model was developed based on the fugacity multimedia model(Mackay et al., 1983; Mackay and Diamond, 1989). A multimedia model based on mass balance equilibrium replacing the fugacity equilibrium, was developed by Kawashima et al. (2007). Unlike realistic pollution treatment, mathematical models can break through spatial limitations and be replicated worldwide. Many researchers have used the fugacity model to simulate different pollutions in different components. By using the level III fugacity model, PAHs (polycyclic aromatic hydrocarbons) were estimated in Dianshan Lake, China (Du et al., 2020) and in the Pacific sector of the Arctic Ocean (Na et al., 2021). Liu estimated the fate of zinc and lead in Lake Ulansuhai, China by using the QWASI model which is also based on the fugacity multimedia model (Liu et al., 2019b). Besides natural environment, multimedia model were developed in order to estimate semi-volatile organic compounds in urban area (Diamond et al., 2001). Csiszar et al. simulated the urban films and film-associated pollutant by using multimedia model (Csiszar et al., 2012). A one-box type multimedia model had been developed and utilized in Lake Biwa-Yodo River Basin to evaluate the risk of Hg emitted from human activity from 1957 to 2007 (Kondo et al., 2013). Studies ranging from modeling macro-scale environmental issues to localized micro-scale environmental assessments can be found in research papers. We can now predict the concentration of environmental chemical pollutions using different mathematical models.

However, these environmental models have their limitations. In most models, the study area was treated as a homogeneous area and the concentration of pollutant was not distributed in space. Also, the emission of pollutant was homogeneous in whole area, these models only use the total emission as the input data. These simplifications and assumptions reduce the accuracy of model results and amplify the uncertainty of subsequent studies based on these data. For the modeling and simulation of pollutants in a specific area most studies are based on the overall average results of the calculations.

The objective concentration gradient over a large area was ignored. The above issues can be better addressed.

Mathematical models have been developed and utilized for various environmental pollutants including organic components and heavy metals. The Level III multimedia model, which is based on fugacity, was developed and applied to organic chemicals by Mackay et al. (1985) and Mackay and Paterson (1991). Various organic chemicals have been used to estimate fate, transport, and steady-state concentrations in the environment using the Level III fugacity model (Edwards et al., 1999). To simulate and predict the fate of heavy metals in lakes and rivers, the QWASI model was developed based on a fugacity multimedia model (Mackay et al., 1983; Mackay and Diamond, 1989). Kawashima et al. (2007) developed a multimedia model based on the mass balance equilibrium replacing the fugacity equilibrium. A generalized compartmental multimedia fate and transport modeling framework was developed for evaluate concentrations of engineered nanomaterials (Liu and Cohen, 2014). Never the less, a multimedia model for environmental assessment of engineered nanoparticles was also developed (Meesters et al., 2014). Several researchers have used these fugacity model to simulate different pollutants in different components worldwide. Using the Level III fugacity model, polycyclic aromatic hydrocarbons were estimated in Dianshan Lake, China (Du et al., 2020) and in the Pacific sector of the Arctic Ocean (Na et al., 2021). Liu et al. (2019b) estimated the fate of zinc and Pb in Lake Ulansuhai, China, using the QWASI model, which is also based on the fugacity multimedia model. In addition to the natural environment, multimedia models have been developed to estimate semi-volatile organic compounds in urban areas (Diamond et al., 2001). Csiszar et al. (2012) simulated urban films and film-associated pollutants using a multimedia model. A one-box type multimedia model was developed and utilized in the Lake Biwa-Yodo River basin to evaluate the risk of Pb emitted from human activity from 1957 to 2007 (Kondo et al., 2013).

These multimedia models have their advantages and limitations shown in Table 1.

Similar to this study, some model considers mass balance by summing all mass

transfers between the four media: equilibrium, emission, advection, and deposition or sedimentation. However, for these models, the study area was treated as a homogeneous area and the concentration of pollutant was not distributed in space. Such as in one-box type multimedia model, the entire study area is assumed as a virtual homogeneous box which divided the space into four different media: atmosphere, water, soil, and sediment. Also, some the emission of pollutant was homogeneous in whole area, these models only receive the total emission as the input data. Although the one-box multimedia model behaved successfully in simulating the Pb concentration (Kondo et al., 2013), the one-box model still has drawbacks, such as the lack of spatial distribution of the concentration in the study area. This is because the model assumes that the Pb concentration in environmental media is homogeneous. The Pb concentration in any location of the Lake Biwa-Yodo River basin is the same without a gradient, which may cause errors in simulation and prediction.

Table 1. Comparison between different multimedia models

Model	**Target substance**	**Property**	**Limitations**	**Reference**
Level III multimedia model	Organic chemicals	Level 3 fugacity approach. Well-mixed compartments. Intermedia mass transport. Equilibrium speciation;	Early version;	Mackay et al. (1985) Feenstra et al. (1991).
QWASI model	Organic chemicals and heavy metals		Homogenous box. Spatial average result without distribution;	Mackay et al. (1983) Mackay and Diamond (1989)
SimpleBox				Meent (1993) Brandes and Den Hollander (1996) Den Hollander and Van de Meent (2004)
One-box multimedia model				Kondo et al. (2013)
SimpleBox4Nano	Engineered nanomaterials	Nonequilibrium colloidal behavior;		Meesters et al. (2014)
MendNano				Liu and Cohen (2014)
Distributional multimedia model (current study)	Organic chemicals and heavy metals	Modified version of Onw-box; Finer mesh; Inner advections;		

1.3 Objective

A well-behavioral environmental fate model can largely help to analyze environmental problems. This study aspires to develop a generalized mathematical model for evaluate environmental pollutants. And based on the result of model, studies about prediction of pollutant concentration and the environmental risk assessments could be carried out. The aim of this study is to develop a multimedia model demonstrating both spatial and temporal distribution of pollutants. The model was inspired by past studies, on which its mechanism and scalability is improved. A one-box type multimedia model had been developed and utilized in Lake Biwa and Yodo River Basin to evaluate the risk of lead emitted from human activity from 1957 to 2007 (Kondo et al., 2013). In one-box type multimedia model, the entire study area is assumed as a virtual box which divided the space into 4 different media, atmosphere, water, soil, and sediment. The model considers the mass balance by sum all mass transfer between 4 media: equilibrium, emission, advection, and deposition or sedimentation. Although the one-box type multimedia model behaved quite well in simulating the concentration of lead (Kondo et al., 2013), it still has demerits such as lacking spatial distribution of the concentration in study area. That is because the model has assumed simply that the lead concentration of environmental media is homogeneous. The concentrations of pollutant in any location of the study area are the same value without gradient. Because the assumption that the concentration of environmental media is homogeneous without any gradient might cause underestimations and overestimations, the one-box type multimedia model can be improved.

Thus, the main objective of this study includes as follow: 1) develop a generalized multimedia model based on one-box type multimedia model which can show the spatial gradient of pollution. 2) apply the generalized multimedia model in a certain study area

to estimate several pollutants in various environmental media 3) validate the model compared with measured data.

1.4 Chapter organization

The chapters in this thesis are organized in the following manner. Chapter 1 provides an introduction of this research which is divided into sections to provide background and objectives. In chapter 2, the methodology is introduced including the computational model and study area, and major data sources. Chapter 3 to 5 describes the main application sections of the model, which is evaluation of different type of pollutants, sulfa-drugs, Pb and Hg. Each chapter include the introduction, detailed methodology of the numerical model, emission estimation of the target substance, calculated results (including the average concentrations in study area and the spatial distribution by simulations), validations, and conclusions, respectively. Chapter 6 summarizes the important conclusions obtained from this study and describe the limitations occurred in the study together with the recommendations for future developments of this research.

2 Methodology

2.1 Multimedia model

2.1.1 Structure of the model

In this research, the generalized distributional multimedia model is developed based on one-box type multimedia model in order to make environmental risk assessment for certain pollutant (Kondo et al., 2013). Some major mechanisms of distributional type model were the same as the one-box type model. Similar to the one-box type model, the distributional model also separates the space into four environmental media, the atmosphere, the soil, the water, and the sediment. The distributional type model first divided the study area into numerous tiny meshes instead of the whole imaginary box in the one-box type multimedia model (Figure 1).

The mass balance of each unit mesh by sum all mass transfer between 4 media (equilibrium, emission, advection, deposition and sedimentation) were simulated separately. Figure 2 showed these mass exchange processes inside each mesh. Furthermore, in distributional multimedia model, the advection process in each mesh considered mass exchanges between its neighbor meshes, while the one-box model only calculated mass exchanges in or out of the whole study area.

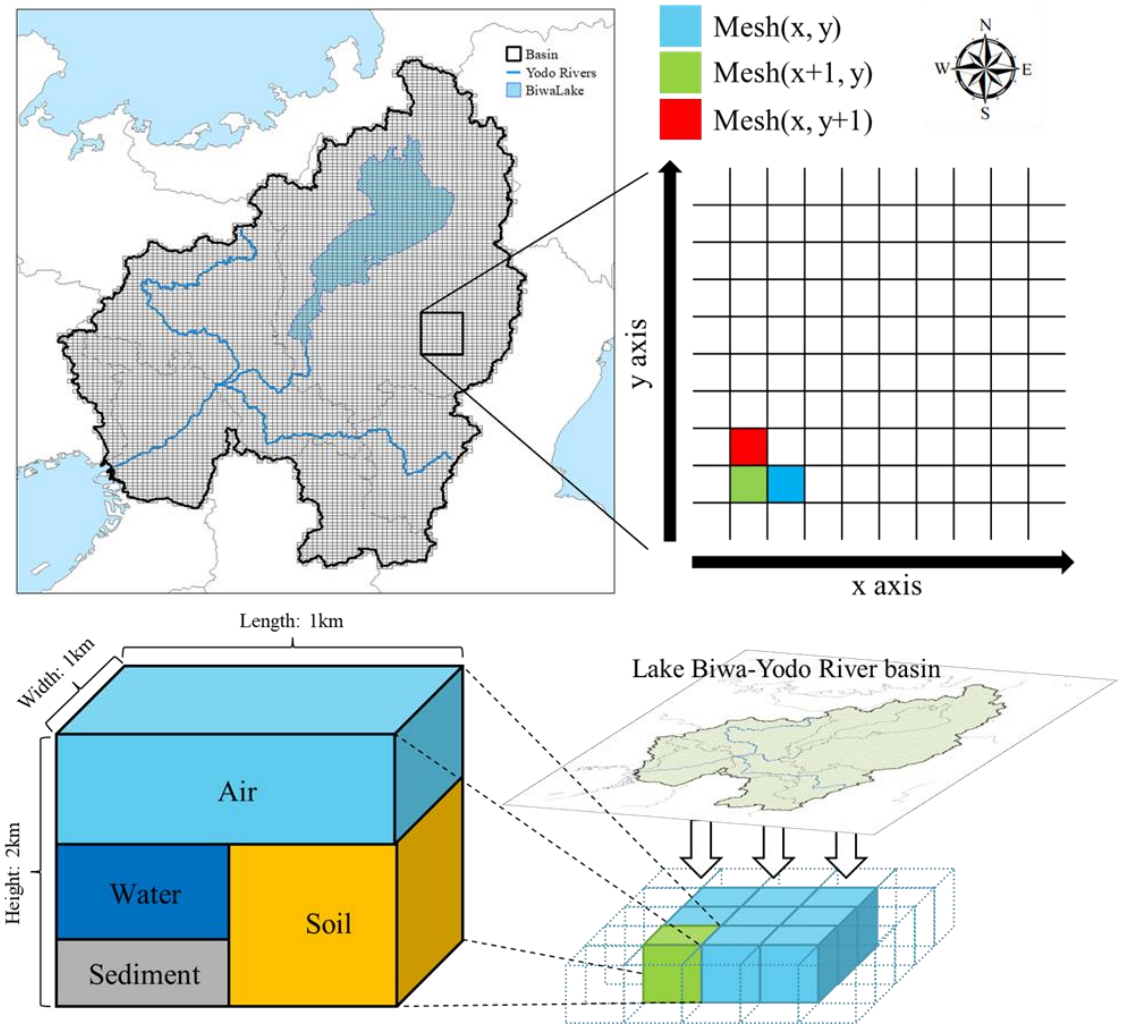

Figure 1. The concept of distributional type multimedia model.

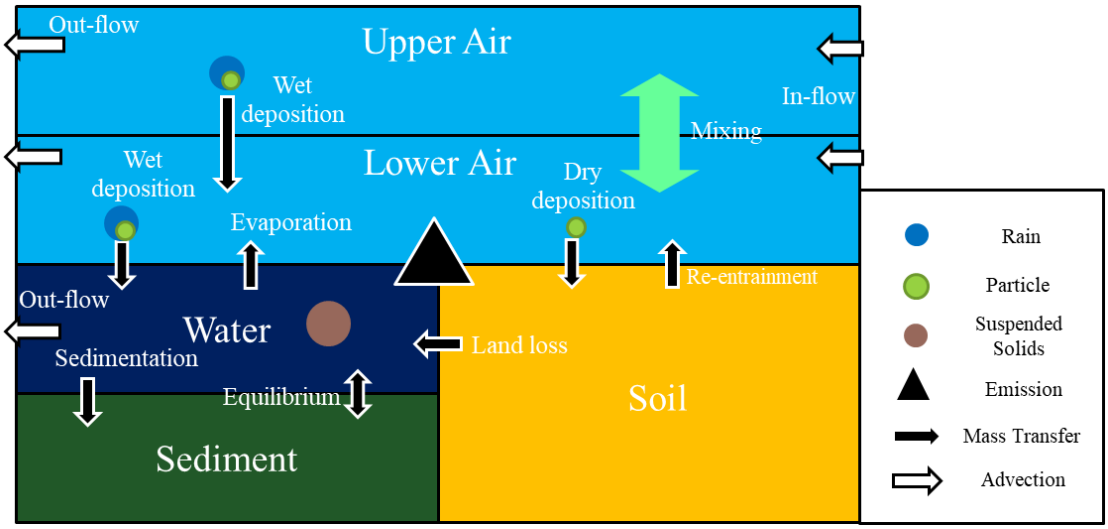

Figure 2. The mass transfer between environmental media.

2.1.2 Basic equations of the model

The main equation of the distributional multimedia model was shown in below.

$$\frac{dM_i}{dt} = f_{e\_i} + \sum_{j=1}^{MN} f_{eq\_ij} + \sum_{j=1}^{MN} f_{dp\_ij} + f_{ad\_i} \quad (1)$$

where *i,j* were the media label number; *MN* was the number of media; *M* means the molar amount of substance; f_{e_i} means the emission flux; f_{eq_ij} means the mass transfer flux between media *i* and *j* due to equilibrium; f_{dp_ij} means the deposition and runoff flux from media *i* to *j*; f_{ad_i} means the advection flux in media *i* affected by other meshes.

In distributional type model, the advection flux was no longer the same value. The advection flux of each mesh was calculated separately, after emission flux, equilibrium mass transfer flux, and deposition flux. The advection flux was affected by adjacent meshes and the mass transfer equation were shown by following.

a) Advections in atmosphere:

$$\frac{dC_{pt}}{dt} = -u\frac{\partial C_{pt}}{\partial x} - v\frac{\partial C_{pt}}{\partial y} \quad (2)$$

where C_{pt} means the concentration in air, *x* is the west-east direction, y is the north-south direction of the mesh, *u,v* are components of wind speed.

b) Advections in the water media.

$$\frac{dC_{wt}}{dt} = -QC_{wt} \quad (3)$$

where C_{wt} means the concentration in the water media of one mesh, *Q* means the discharge of the water.

c) Advections in the suspended solid media.

$$\frac{dC_{ss}}{dt} = -QC_{ss} \quad (4)$$

where Css means the concentration in suspended solid phase, Q means the discharge of the water.

The advections in air include inflows from adjacent meshes in 4 directions (north, south, west, east) and outflows to the adjacent meshes, depending on the wind speed. The

advections in water include inflows from upstream meshes (up to 4 directions, north, south, west and east) and outflow to downstream mesh, depending on the water flow direction.

2.1.3 Mass transfers

The generalized distributional multimedia model considered many chemical phenomena, including the emission, degradation, atmospheric mixing, deposition (dry and wet), sedimentation, re-suspension and advection. In some case of the chemical substance, particles or ion exchange was take into consideration.

- Emission

  This phenomenon represents major source of a certain substance. The pollutant caused by human activities was discharge into the environment, especially into atmosphere, soil, and water. This reflects the direct impact of human activities on the environment. In some case, natural emission caused by natural processes such as soil erosion and natural transformation into other chemical compounds also can occurred, rather than human activities.

- Degradation

  In this study, degradation is a major process that removes the chemical. Degradation is the processes of natural decaying, accumulated into living organisms via their consumption and conversion of chemicals into various other chemical compounds in the environment (Seinfeld J.H. and Pandis S.N., 2006). For one certain chemical substance, conversion or breaking down is the process of removal, but for another chemical substance, it is also an emission process.

- Atmospheric mixing

  In distribution multimedia model, the atmosphere was divided into 2 vertical parts,

the upper and the lower layer. The atmospheric mixing height (height of the lower layer) changes from 200 m to 1000 m from the sea level hourly. This process represents the movement of chemicals between two layers.

- Deposition

  This is the process chemicals in the atmosphere deposit themselves on soil or on water body. The deposition includes wet deposition caused by the precipitation and dry deposition such as natural settlement due to the gravity. Wet deposition transfers chemicals in gases or particle phase to the ground in an aqueous form (such as rain, snow or fog) via processes of precipitation. In this process, atmospheric hydrometeors catch the chemicals and deposit them on soil or water body. Dry deposition transfer chemicals in both the gases and particulate phase on soil or on water body without the aid of precipitation (such as gravitation, interception, impaction, and turbulence) (Seinfeld J.H. and Pandis S.N., 2006).

- Sedimentation

  Sedimentation mainly occurs in water media. Suspended solids (SS) in the water settle down on the bottom of the water body due to gravitation and these SS can absorb various chemicals and then facilitate the transportation of them to the soil at the bottom of the water body

- Re-suspension

  This is the reverse process where the chemicals are released into the water body as SS from the sediment.

- Advection

  This process refers to the transport of chemicals from one region to another due to the movement of the air or water. Normally, advection in atmosphere can occur

vertically and horizontally. In this study, only the horizontal movement from one region to another due to the wind currents is considered as advection, while the vertical movement is regarded as atmospheric mixing. In water media, chemicals move due to the water flow (Seinfeld J.H. and Pandis S.N., 2006).

- Particles and ion exchange

  Only in the case of chemicals which has form of particle and ion, this process is considered. This process occurs between the particle phase and ionic phase. This process can occur within the same environmental media (intra media exchanges) or between different environmental media (inter media exchanges). An example of intra media exchanges is chemical exchanges between the SS and the water due to molecular diffusions and charge attraction. Also, atmospheric hydrometeors (such as rain or snow) may dissolve or ionizes the chemicals in form of particles. The inter media exchanges can occur when the particle of chemicals in atmosphere drop into water surface due to dry deposition, and when the particle in soil run into water body.

2.2 Variables

In distributional type multimedia model, variables used in one-box type model (Kondo et al., 2013) were modified and new variables were added. Modifications are shown in the following:

- Mass transfers between/in environmental media.

  Because the study area was divided into serials of unit mesh, material exchange between different media (inter media exchanges) were separated and labeled with x (west-east direction) and y (north-south direction). In detail, each variable was represented by a two-dimensional array.

- The mass transfer in the atmosphere by adjacent meshes.

Concentration of each mesh in atmosphere were affected by meteorological phenomenon (wind) from adjacent meshes in four directions (north, east, south and west).

- The mass transfer in the water by adjacent meshes.

  Concentration of each mesh in water media were affected by the upstream mesh if there was a river across that mesh geographically.

- The distribution of total emission.

  The emission of substance in each mesh were estimated separately and labeled with x (west-east direction) and y (north-south direction).

Considering above modifications, the main variables describe the gross mass in each media used in distributional model was reconstructed using two-dimensional arrays which identify the mesh position in study area. Each variable was labeled with the subscript [x, y], where x means the west-east order, and y means the north-south order.

2.3 Study area

2.3.1 Lake Biwa-Yodo River basin

In this research, the Lake Biwa-Yodo River basin was selected as the target area to investigate the environmental risk of different chemicals, using the distributional multimedia model. The Lake Biwa-Yodo River basin is one of Japan's representative water systems in the Kinki region of Japan (Figure 1), whose main river has 75 km channel length and the total area is of 8,240 km2, including Osaka, Hyogo, Kyoto, Shiga, Nara and Mie prefectures (Yodogawa River Office). The basin has the largest freshwater lake Lake Biwa and is the oldest lake in Japan with a history of approximately four million years and is also one of the 20 ancient lakes in the world (Shiga Prefectural Government). Lake Biwa is located in Shiga Prefecture with an area of 669.26km^2 and the storage

capacity is around 27.5 billion m^3 water and can be subdivided into South Lake Biwa and North Lake Biwa with an area proportion of 1 to 11 (Shiga Prefectural Government).

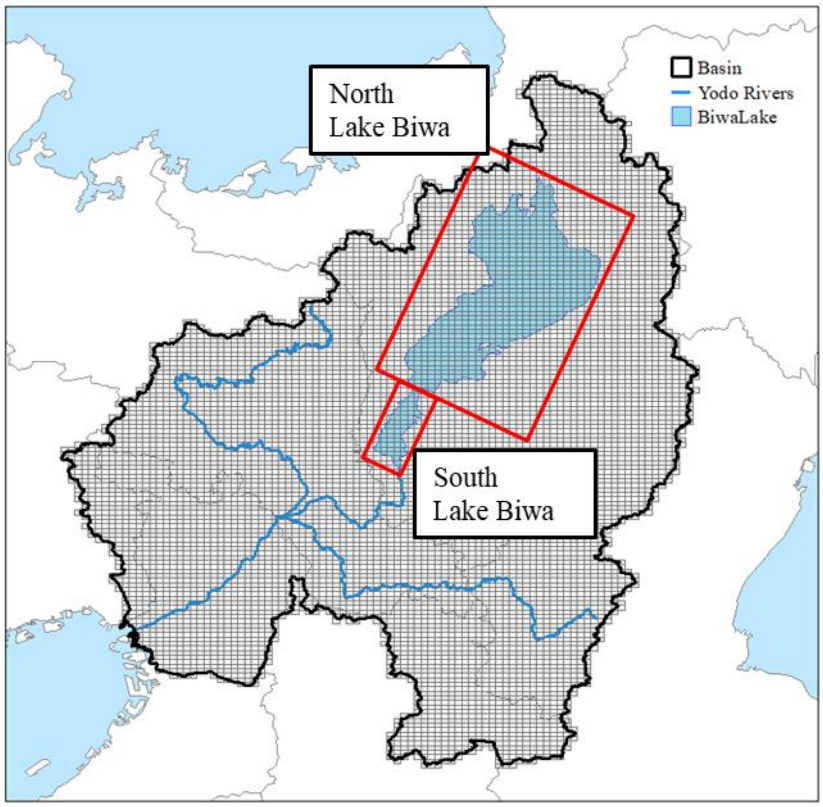

Figure 3. The structure of Lake Biwa.

It has a valuable natural environment, boasting more than 60 endemic species, and is indispensable for the livelihoods and industrial development, supporting the social, economic and cultural foundations of the Kinki region. The population of the basin account for more than 9% of the total population of Japan, including large cities such as Kyoto and Osaka and their surrounding satellite cities (Lake Biwa-Yodo River Water Quality Preservation Organization) and reached approximately 12.1 million in 2020. Harmful chemicals have been discharged into the environment around this famous and historical basin area. It is necessary to evaluate environmental risk in Lake Biwa-Yodo River basin due to its unique location and great industrial value.

2.3.2 Mesh division

In distributional multimedia model, each calculate unit was constructed with 1km width, 1km length and 2km height space. Figure 1 visually explains the division of the Lake Biwa-Yodo River Basin. Every unit mesh was labeled with x and y each represent the order of horizontal (west-east) axis and vertical (north-south) axis respectively. The total number of meshes in Lake Biwa-Yodo River basin was 8775 including 428 boundary meshes.

2.3.3 Special mesh

Meshes located inside the Lake Biwa cannot use the water advection equations (2-3) directly because the water flow direction between these meshes are too complicated. Thus, in this study, the North Lake Biwa and the South Lake Biwa were separated and considered as two special unit meshes. Figure 4 shows the structure of these meshes. Some simplifications were made in this study:

- Independent variables were used to represent the concentration of these meshes located inside the North Lake Biwa or South Lake Biwa. The concentration of chemical substance in water media share the same value.
- North Lake Biwa and South Lake Biwa had several neighboring upstream meshes which located outside of the lake because some river finally flow into the unit mesh.
- The North Lake Biwa was the upstream mesh of the South Lake Biwa.
- The South Lake Biwa was the upstream mesh of the River Yodo.

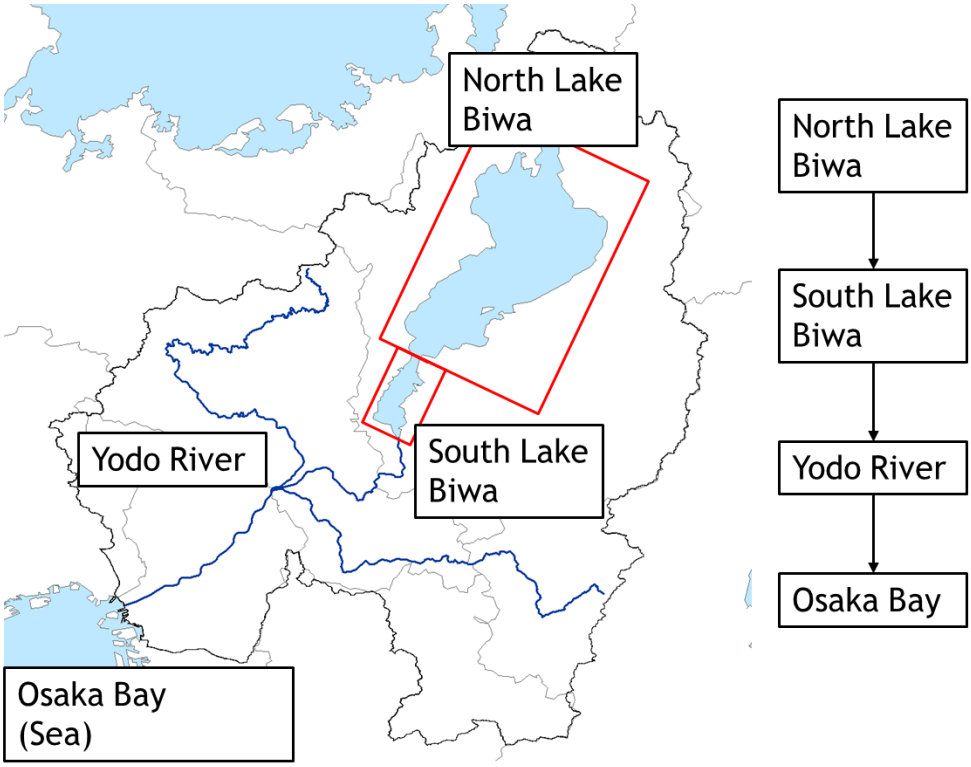

Figure 4. The structure of Lake Biwa.

2.4 Common input data

2.4.1 Wind

The advection in atmosphere within the Lake Biwa-Yodo River basin was calculated by using the wind data. The wind data was from the Meso-Scale Model published by the Japanese Meteorological Agent (Japan Meteorological Business Support Center). The GPV-MSM covered Japan and surroundings of 22.4 to 47.6 degrees north latitude and 120 to 150 degrees east longitude, with three hour intervals, horizontal resolution of 0.05° × 0.0625° on the ground surface and 0.1° × 0.125°, maintained by Japan Meteorological Agency. The pressure surface was divided into 16 layers (100, 150, 200, 250, 300, 400, 500, 600, 700, 800, 900, 925, 950, 975, 1000 hPa), including geopotential altitude, North and South components, temperature, rising flow, relative humidity data. The ground surface data including sea surface refining pressure, ground pressure, wind speed east-

west or north-south component, temperature, relative humidity, time precipitation, cloud amount. In this study, wind speed and direction data in 2009 was calculated as an average value of atmospheric pressure surface of 900 to 1000 hPa.

In distributional multimedia model, wind data with mass outliers such as extreme weathers should be avoid because the focus point was the long-term behavior evaluation over decades. Thus, the meteorological data used in this study contains u and v components of wind speed every 3 hours in the year 2010, which the weather situation were stable without typhoon. The wind speed data were repeated every year during the whole simulation period and reset at the beginning of each year.

2.4.2 Precipitation

The wet deposition between atmosphere and water media were heavily affected by the precipitation. The data used in this study was calculated based on assessment of the water resource of the Yodo River Basin (Shrestha and Kondo, 2015). Same to wind data, the data contained the hourly precipitations of each mesh in year 2010 in order to keep the resistance and improve the accuracy. During the simulation, the precipitation of each mesh was reset at the beginning of the year and repeated every year (Figure 5).

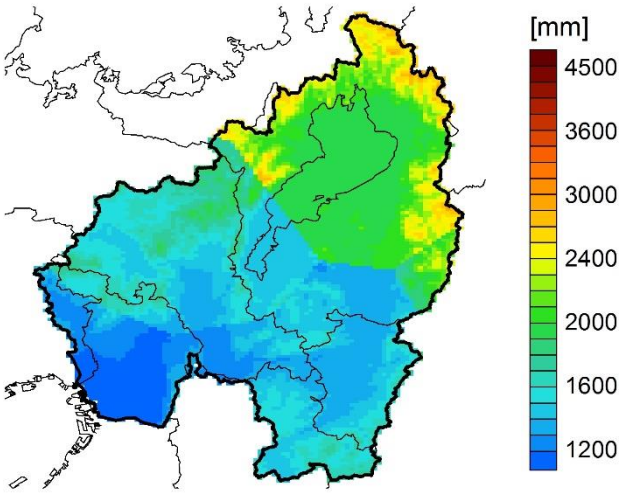

Figure 5. Precipitation of mesh in Lake Biwa-Yodo River basin.

2.4.3 River discharge

In distributional multimedia model, the water advection inside the Lake Biwa-Yodo River basin was taken into consideration. Flow direction and hourly river quantities of each mesh in the study area were used as an input data which was calculated based on the distributed hydrological model (Figure 6) (Kojiri et al., 2008) and river discharge simulations (Shrestha and Kondo, 2015). The water flow direction of each mesh was determined with the rivers in the basin (Figure 3). The detail was figured out by followings: A) The direction of any mesh where river crossed was the same as the perennial river flow. B) The direction of mesh where no river across was decided directly by the altitude.

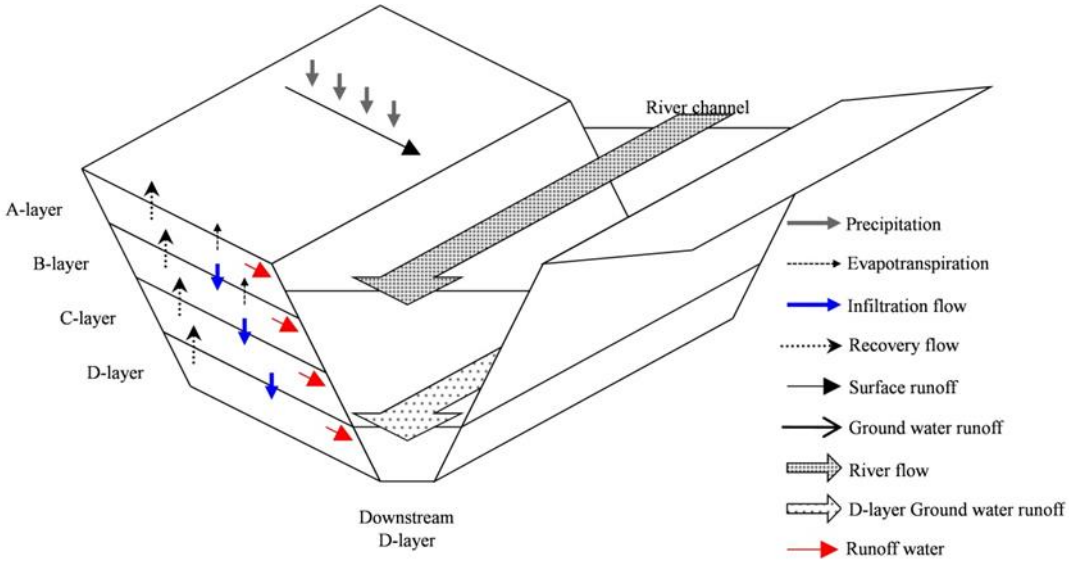

Figure 6. Overview of Hydrology model.

2.5 Calculation process

Figure 7 shows the process of distributional multimedia model. The mass transfer was deal first, after inter media exchanges, the mass transfer between neighbor meshes occurred.

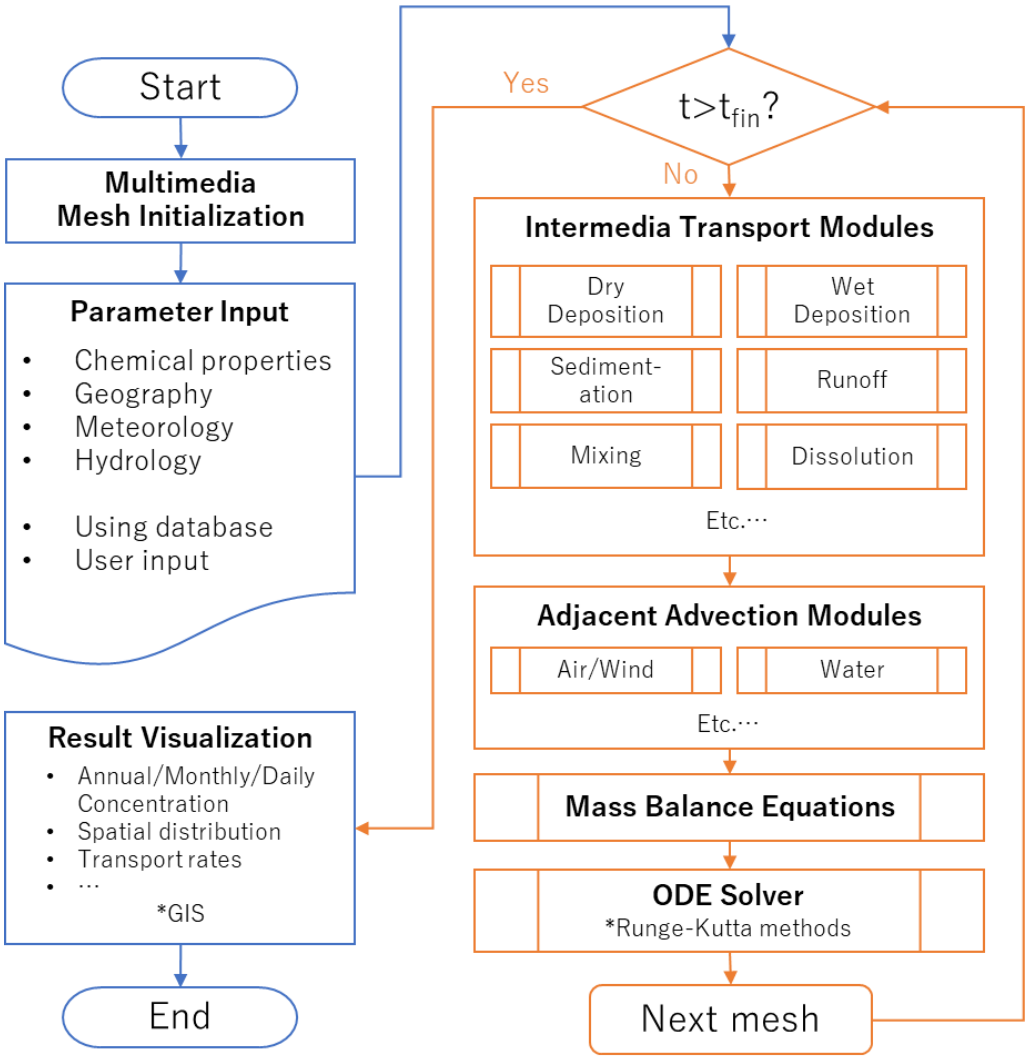

Figure 7. The calculation flow of distributional multimedia model.

3 Apply to lead

3.1 Introduction

Lead (Pb) has been widely used from ancient ages because of its physical properties such as easy processability. As one of the raw materials during chemical industries, Pb was used for such as battery, metal pipes, cable sheathing and radiation protection and are considered as priority heavy metals that could pose environmental health risks (Wuana and Okieimen, 2011). However, lead poisoning is a public environmental problem and health hazard (Rabinowitz and Needleman, 1982) which the history of poisoning even reached nearly 2,500 years (Hernberg, 2000). For instance, the concentrations of Pb in environmental media are associated with children's blood lead levels (Angle et al., 1984; Roper et al., 1991; Lanphear et al., 1998).

However, monitoring environmental Hg in a large geographical region is not very practical. It is impractical to arrange for a large number of detectors to regularly measure environmental concentrations over such a large area, and simultaneous measurements at multiple locations cannot be achieved. Also, it would be uneconomical to collect data periodically by setting up measuring equipment in that area. Considering the practical difficulty in monitoring and the adverse health effects of Hg such as carcinogenicity, child developmental defects, and toxic effects on nervous, digestive, and immune systems (Organization;), it is important to evaluate the concentration of Hg using environmental modeling.

3.2 Methodology

3.2.1 Modifications

In distributional type multimedia model, variables used in one-box type model were

modified and new variables were added. Modifications are shown in the following.

(I) Exchange of lead particles and ions between/in environmental media.

Because the study area was divided into serials of unit mesh, material exchange between different media (inter media exchanges) were separated and labeled with x (west-east direction) and y (north-south direction). In detail, each variable was represented by a two-dimensional array.

(II) The chemical transport in the atmosphere by adjacent meshes.

Lead concentration in atmosphere of each mesh were affected by meteorological phenomenon (wind) from adjacent meshes in four directions (north, east, south and west).

(III) The chemical transport in the water by adjacent meshes.

Lead concentration of each mesh in water were affected by the upstream mesh if there was a river across that mesh geographically.

(IV) The distribution of total emission.

The emission of lead in each mesh were estimated by proportion according to the land-use data.

Figure 8 shows the mass exchange processes, including emission, deposition, advection, and sedimentation inside each mesh, which were the same as the one-box type mode. The details of these mass balances and transfers among the four environmental media are described in a one-box multimedia model (Kondo et al., 2013). Furthermore, in the distributional type model, the advection process in each mesh considered mass exchanges between its neighbor meshes, while the one-box model only calculated mass exchanges in or out of the whole study area.

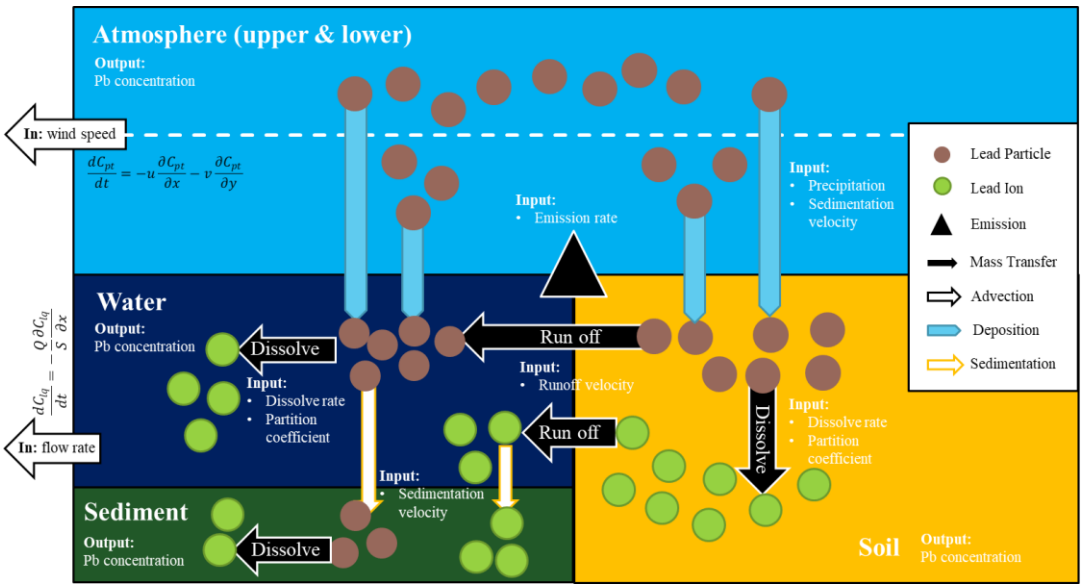

Figure 8. The mass transfer between environmental media.

3.2.2 Simulation period

In this study, we estimated Pb emission in Lake Biwa-Yodo River basin to simulate the accumulation of Pb from 1957 to 2016. In distributional multimedia model, the simulation result was affected by the initial value. However, there were less data represent the initial Pb concentration in year 1957. In order to improve the accuracy of the results, the simulation started at 1945 with a 12 years run-up period. The concentration in the end of the run-up period was regarded as the initial value for the rest time.

3.2.3 Variables

Considering above modifications, the main variables describe the gross mass of lead in each media used in one-box type model (Kondo et al., 2013) was reconstructed using two-dimensional arrays. Each variable was expanded into two-dimensional array and the subscript [*x, y*] means the west-east order of mesh is *x*, and the north-south order is y. Table 1 shows the total amount of the substance to be calculated in each media *M* (unit: mol), and total eight variables. In distributional type multimedia model, the mass transport between neighbor meshes occurred after the inter media exchange.

Table1. Main variables in distributional multimedia model

Mptu[x,y]	Total amount of lead particle in upper atmosphere.
Mptd[x,y]	Total amount of lead particle in lower atmosphere.
Mslpt[x,y]	Total amount of lead particle in soil. (solid phase)
Msllq[x,y]	Total amount of lead adsorbed in soil. (liquid phase)
Mss[x,y]	Total amount of lead particle as suspended solid.
Mwt[x,y]	Total amount of lead in water.
Msdpt[x,y]	Total amount of lead particle in sediment. (solid phase)
Msdlq[x,y]	Total amount of adsorbed lead in sediment. (liquid phase)

3.2.4 Other simplifications

Akitomo el al. once performed a model experiment to investigate the annual cycle of circulations in Lake Biwa (Akitomo et al., 2009). According to their study, Lake Biwa maintained the system of multiple gyres. The water flow changes among different time period. Even in their model, there are some discrepancies between the simulated and observed water temperature and velocity fields. The meshes located inside Lake Biwa cannot use the water advection equations (2–3) directly because the water flow direction between these meshes is too complicated. Thus, in this study, North Lake Biwa and South Lake Biwa were separated and considered as two special meshes. Simplifications have been made as following: Independent variables were used to represent the Pb concentration of the North Lake Biwa and South Lake Biwa. Some rivers finally flowed into these two meshes. The North Lake Biwa was the upstream mesh of the South Lake Biwa and the South Lake Biwa was the upstream mesh of River Yodo.

3.3 Emission estimation

3.3.1 Introduction

The distribution of Pb emission was estimated base on the total estimation of the Lake

Biwa-Yodo River basin in one-box type model (Kondo et al., 2013). In this case of study, the major emission data was from the Pollutant Release and Transport Registry (PRTR) system. The PRTR system requires business operators to submit notifications regarding specified chemical substances that may be harmful to human health and ecosystems to their regional or municipal governmental authorities (Ministry of Economy Trade and Industry, 2001). Business operators report their own emissions into the environment during the previous year once a year. The relevant government ministry then collates the notified data and calculates the total of reported emissions and makes all information publicly available.

The distribution also calculated on different sources; Registered emission (large industries and large sewage lines) and Unregistered emission in PRTR (small industries, small sewage lines and paint), Leaded gasoline, Incinerator and Painting. Different emission source was estimated specifically by followings.

3.3.2 Emission based on PRTR

In this part, the distribution of Pb emission was estimated by the PRTR report data in 2007. The emission of the whole simulation time (from 1945 to 2016 including 12 years run-up period) was proportion of the estimation result in year 2007. The distribution of two type data from PRTR report maintained by Japanese government was estimated by:

- Every PRTR-registered establishment (including the sewer industry) distributed the amount of Pb emission to the mesh where the establishment located.
- The distribution of other PRTR-unregistered emissions was based on Land utilization tertiary mesh Data published by Japan government (Ministry of Land Infrastructure Transport and Tourism, 2022). The data consisted classifications (paddy field, field, orchard, forest, waste area, building use, trunk transportation land, lake, river, etc.)

in tertiary mesh units (1 km meshes) based on status of nationwide land usage. Unregistered emissions were allocated in proportion to the building ratio of each mesh.

3.3.3 Emission caused by paints

The uses of paints were roughly divided into three types: paint used in construction, paint for structures and road marking paint. In this study, the total amount of Pb emitted from paint was estimated based on the usage of paint in year 2007 published by the Ministry of the Environment. The emission inside the Lake Biwa and Yodo River basin was multiplied by the percentage of the population in the basin. Pb emission in other years was estimated by followings:

- Pb emission from building paint and structural paint was proportion of the shipment of paint in that year (Japan Paint Manufacturers Association).
- The emission from road marking paint was proportional to the distance of road in the basin (Ministry of Land Infrastructure Transport and Tourism).

However, as accurate data on paint shipments are only available up to 1978, the average value for 1978-1982 was used for years prior to 1977. The distribution of Pb emission from paint was also estimate separately based on the building area ratio and transportation area ratio of mesh from the Land utilization tertiary mesh Data (Ministry of Land Infrastructure Transport and Tourism, 2022):

- The emission from paint used in construction and structures were distributed in proportion to the building area ratio of each mesh (Figure 9).
- Emission from road marking paint was distributed in proportion to the road area ratio of each mesh (Figure 10).

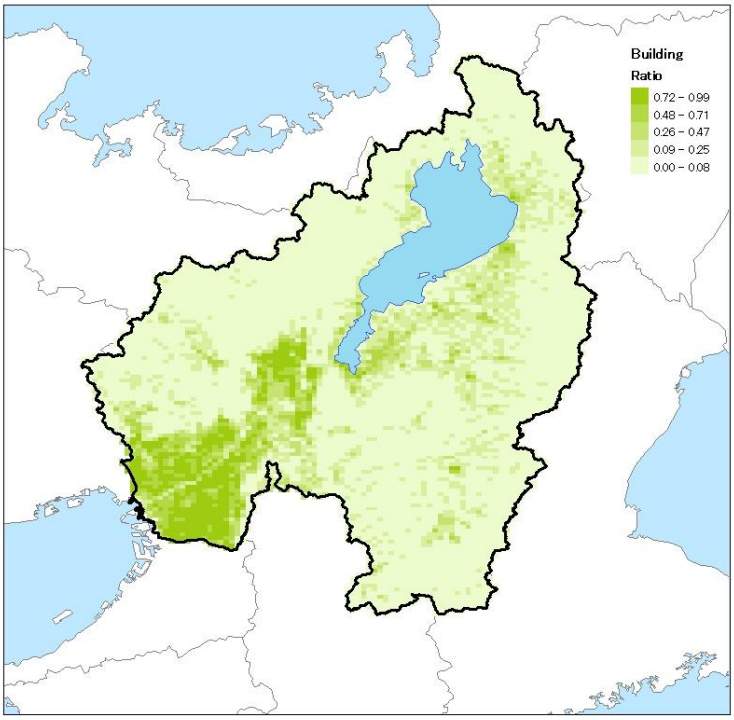

Figure 9. Building area ratio of each mesh.

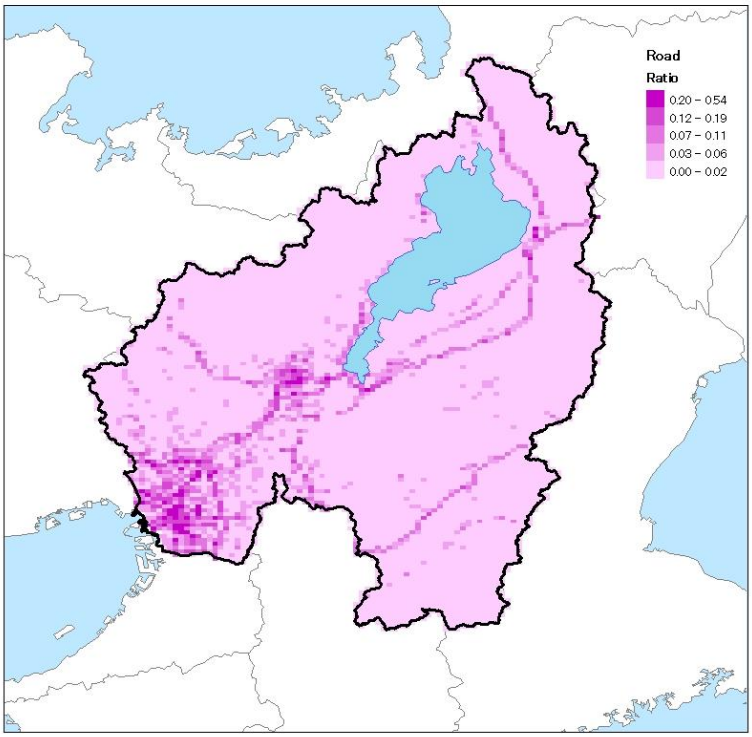

Figure 10. Road area ratio of each mesh.

3.3.4 Emission caused by leaded gasoline

Pb particles from leaded gasoline was assumed to be emitted to atmosphere by the combustion. In Japan, the regular leaded gasoline and the high-octane gasoline was changed into unleaded in 1975 and in 1983. All gasoline consumption became unleaded in Japan after 1987. The total Pb emission was estimated based on the gasoline consumption and the content rate of Pb to gasoline multiplied by the national usage of gasoline. The emission inside the basin were multiplied by the population proportion of the national population.

The distribution of gasoline emission was proportional to the NO emissions from motor vehicles. The NO emission data for each mesh was based on the data of East Asian Air Pollutant Emissions Grid Database, EAGrid2000-Japan (Center for Global Environmental Research). The EAGrid2000-Japan is a detailed inventory for the Japanese region developed as part of EAGrid2000, which was developed as an input to a long-range atmospheric transport model for the East Asian region (FUKUI et al., 2014). The data are maintained at a horizontal resolution of approximately 1 km x 1 km for the whole of Japan, with the base year set to 2000 and 24-hour variations considered by month and by weekday and holiday.

3.3.5 Emission caused by incineration process

Most Pb particles emitted from incinerators are trapped as burned ash and finally buried. Pb emissions from incinerator to atmosphere were calculated based on the national lead emissions from municipal solid waste landfills from 1976 to 2005 (Norihiro Kobayashi and NAITO Wataru, 2006). The emission inside the Lake Biwa and Yodo River basin are equal to the national emission multiplied by the population ratio. Since there was not enough data about the installation of dust collectors, the emission before 1976 was assumed to be the same emissions as in 1976. Also, the emission after 2005 was assumed

to be the same as in 2005. Emissions from incinerators were distributed to every mesh according to the address of each incinerator in the Lake Biwa-Yodo River basin.

3.3.6 Result and distribution of emissions

Figure 11 shows the total annual emissions of the Lake Biwa-Yodo River basin and the proportion of discharge destination (to the atmosphere, water, and soil) from 1957 to 2016. Maximum Pb emissions occurred in 1969. Subsequently, Pb emissions decreased. Figure 12 shows the distribution of the total lead emission (added up with discharge sources) to different environmental media in the year of their maximum value. It was found that the emissions were concentrated in the southern part of the Lake Biwa-Yodo River basin where the urban city are located. And the emission of meshes where rivers cross through (Figure 3) were also high. High road ratios of these meshes caused more leaded-gasoline usage and vehicle exhaust emission. High building ratios of these meshes meant there were more human activities and cause more Pb emission during the PRTR system.

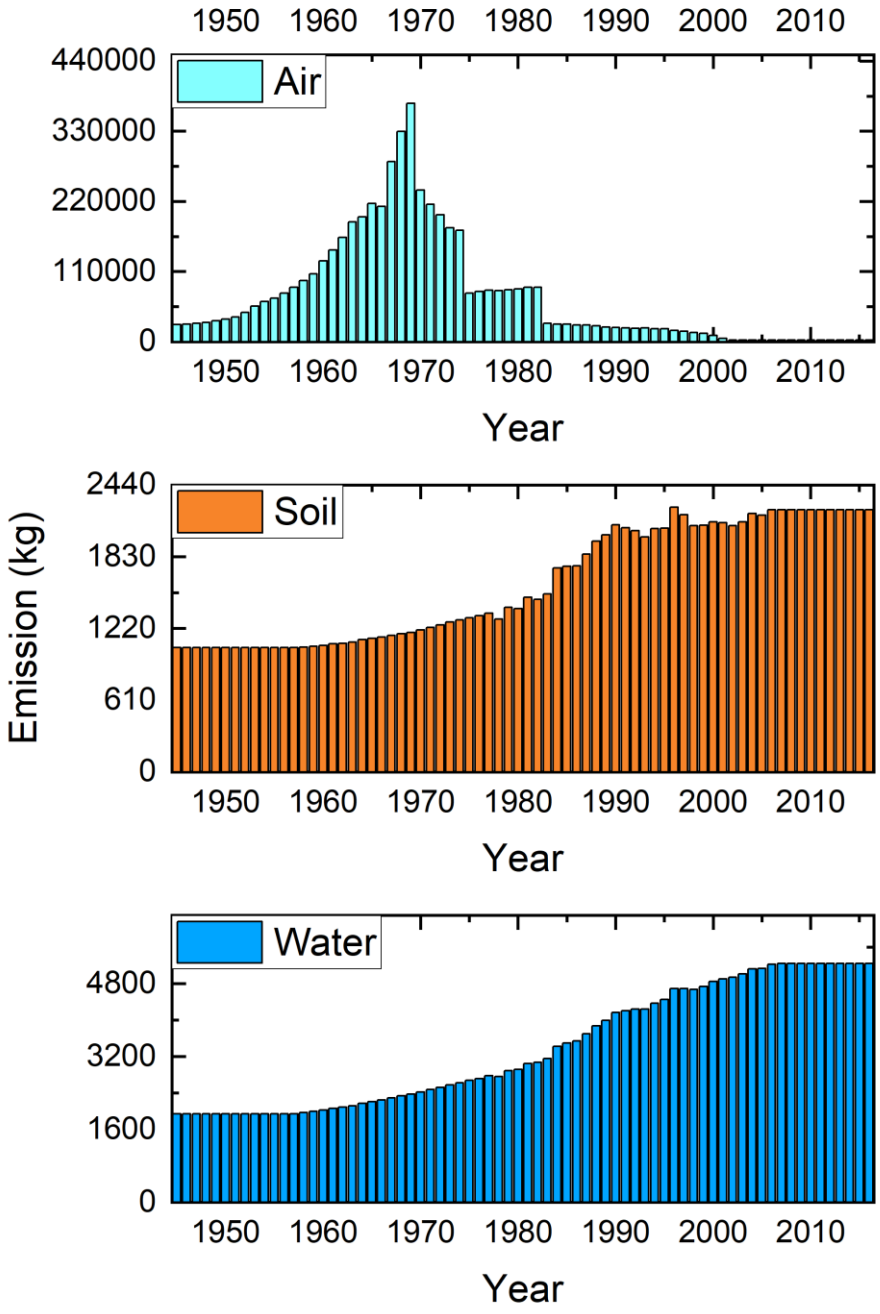

Figure 11. Annual Pb emission to different environmental media.

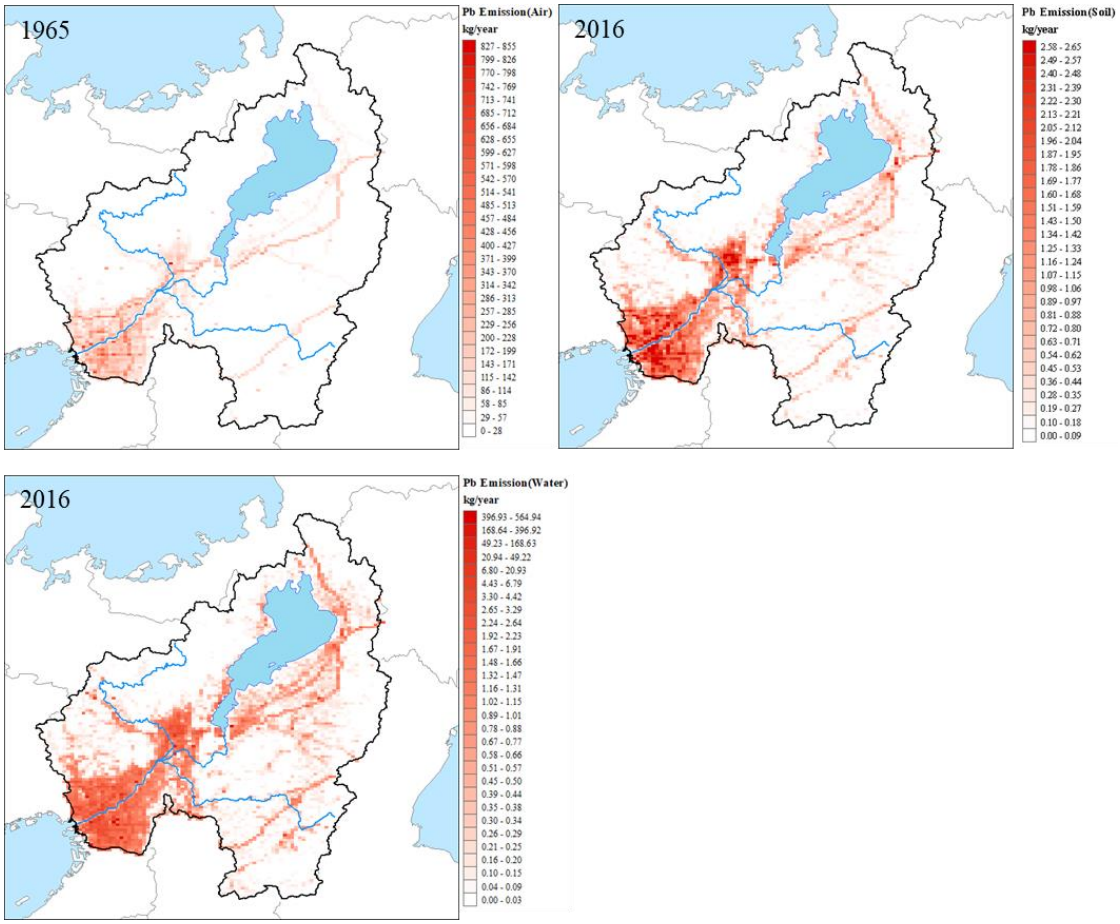

Figure 12. Distribution of Pb emission of each media.

3.4 Result

3.4.1 Annual Pb concentration

Distributional multimedia simulated the concentration of Pb in the annual Lake Biwa-Yodo River basin from 1957 to 2016. The annual variation in the Pb concentration in each medium (atmosphere, soil, water, and sediment) from 1957 to 2016 is shown in Figure 13. The concentration was the spatial average value of the entire study domain, the Lake Biwa-Yodo River basin. The calculated concentration in air was compared with measured data. The concentration in the atmosphere increased until 1969, but rapidly decreased in 2002 due to a sudden decrease in emissions to the atmosphere. The concentration in the sediment and soil showed a slightly increasing tendency, while the rate of increase

decreased after 1969. In addition to the overall year-by-year trend, we compared the simulated and observed values for 2005, which shown in Figure 14. The observation data was compared with the spatial average Pb concentration of whole Lake Biwa-Yodo River basin. Overall, the spatial average simulated values of the study area were underestimated, especially in the atmosphere and in the soil. The mean squared error reached 1.2 $x10^{-20}$, 0.029, 2.5 $x10^{-11}$ and 0.0028 in four environmental media (atmosphere, soil, water, sediment). This was because the spatial average values ignored the concentration gradient of Pb. The sampling locations for observation were located in areas of high concentrations. Nevertheless, the simulations in water and sediment media could reflect the measured values.

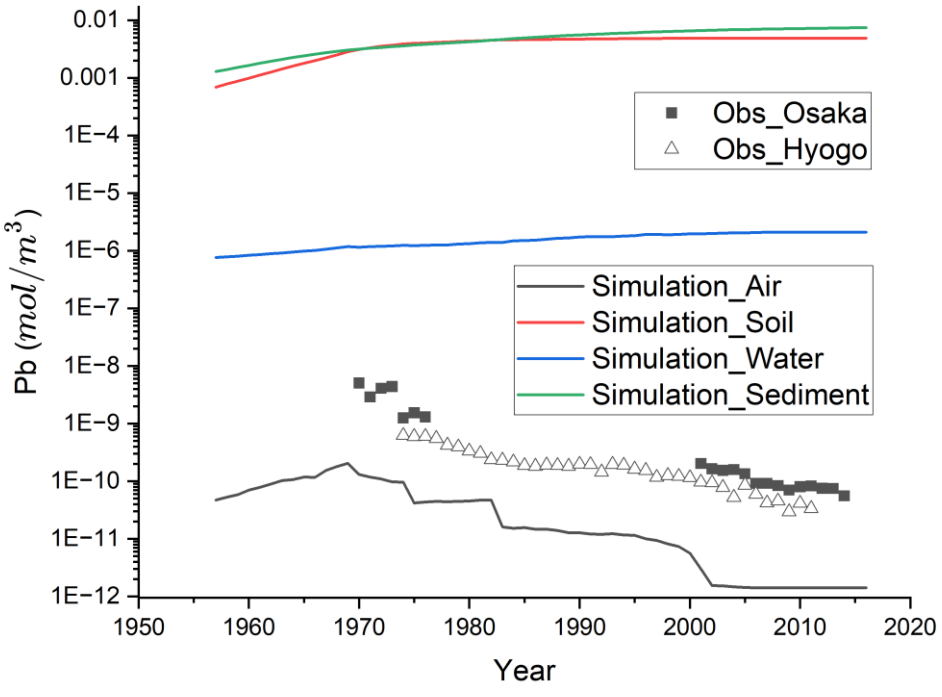

Figure 13. Simulation in different media from 1957 to 2016 and observation in Lake Biwa-Yodo River basin.

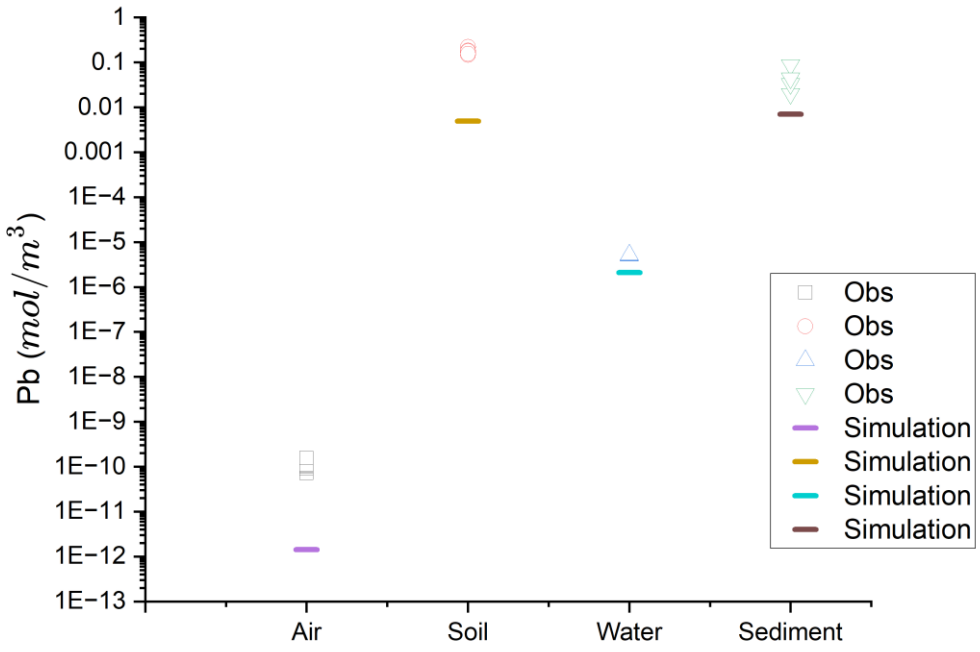

Figure 14. Observation and simulation of different media in Lake Biwa-Yodo River basin (2005).

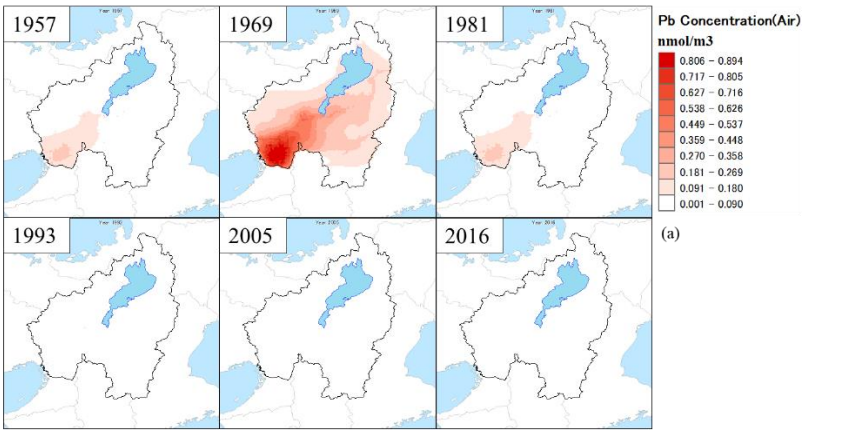
1957
1969
1981
1993
2005
2016
Pb Concentration(Air)
nmol/m3
0.806 – 0.894
0.717 – 0.805
0.627 – 0.716
0.538 – 0.626
0.449 – 0.537
0.359 – 0.448
0.270 – 0.358
0.181 – 0.269
0.091 – 0.180
0.001 – 0.090

(a)

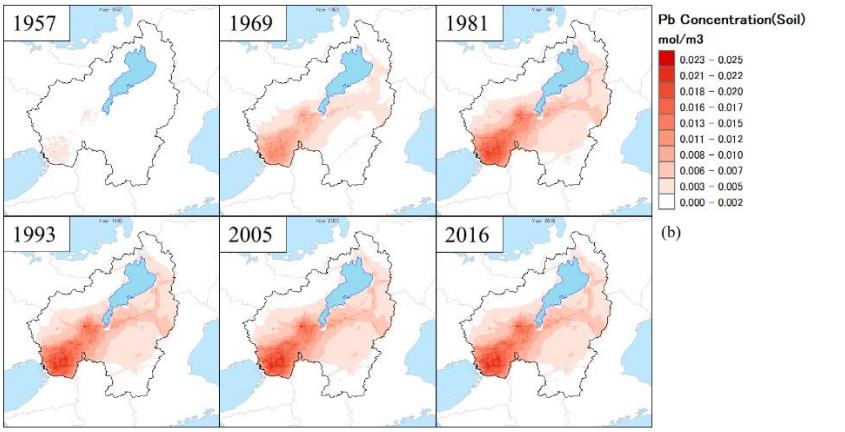
1957
1969
1981
1993
2005
2016
Pb Concentration(Soil)
mol/m3
0.023 – 0.025
0.021 – 0.022
0.018 – 0.020
0.016 – 0.017
0.013 – 0.015
0.011 – 0.012
0.008 – 0.010
0.006 – 0.007
0.003 – 0.005
0.000 – 0.002

(b)

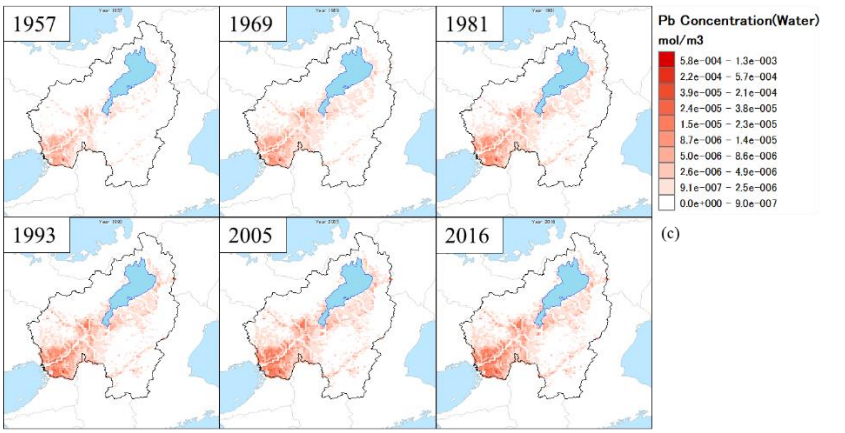
1957
1969
1981
1993
2005
2016
Pb Concentration(Water)
mol/m3
5.8e-004 – 1.3e-003
2.2e-004 – 5.7e-004
3.9e-005 – 2.1e-004
2.4e-005 – 3.8e-005
1.5e-005 – 2.3e-005
8.7e-006 – 1.4e-005
5.0e-006 – 8.6e-006
2.6e-006 – 4.9e-006
9.1e-007 – 2.5e-006
0.0e+000 – 9.0e-007

(c)

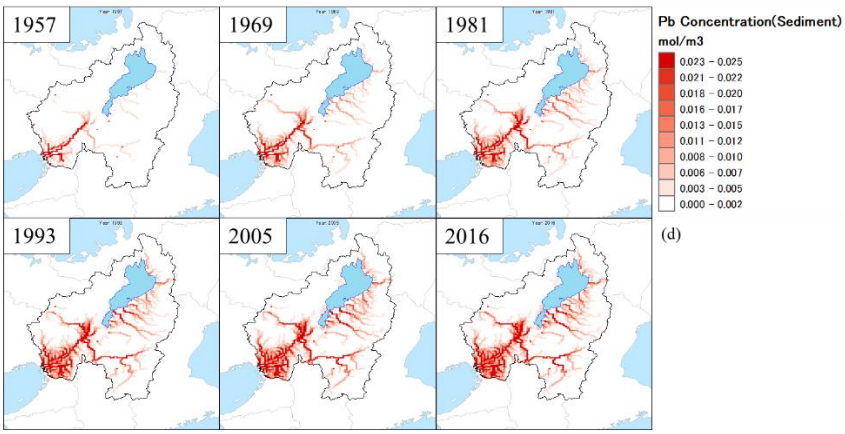
1957
1969
1981
1993
2005
2016
Pb Concentration(Sediment)
mol/m3
0.023 – 0.025
0.021 – 0.022
0.018 – 0.020
0.016 – 0.017
0.013 – 0.015
0.011 – 0.012
0.008 – 0.010
0.006 – 0.007
0.003 – 0.005
0.000 – 0.002

(d)

Figure 15. Spatial Pb distribution of different media in 1957, 1969, 1981, 1993, 2005 and 2016.

3.4.2 Pb in atmosphere

To evaluate the model results, this study selected several observational data with Pb concentrations in the atmosphere from the government's report. The location of observation points in Hyogo and Osaka were shown in Figure 16. The observational data of Hyogo was from one observation point, and data of Osaka was the average value of four points. Figure 13 shows the special average Pb concentration in the atmosphere calculated using the distributional multimedia model compared to the observational data. The simulated concentration in the atmosphere was comparatively lower than the observed concentration, the mean squared error was 1.25 $x10^{-18}$. Similar to the one-box multimedia model result, the Pb concentration in the entire Lake Biwa-Yodo River basin increased from 1957 to 1969 owing to the increase in Pb emissions from vehicle gasoline. Since 1969, the concentration has shown a downward trend along with a decrease in total emissions. It was also shown that two rapid reductions occurred because of the prohibition of leaded gasoline in 1975 and effluent control in the 1990s.

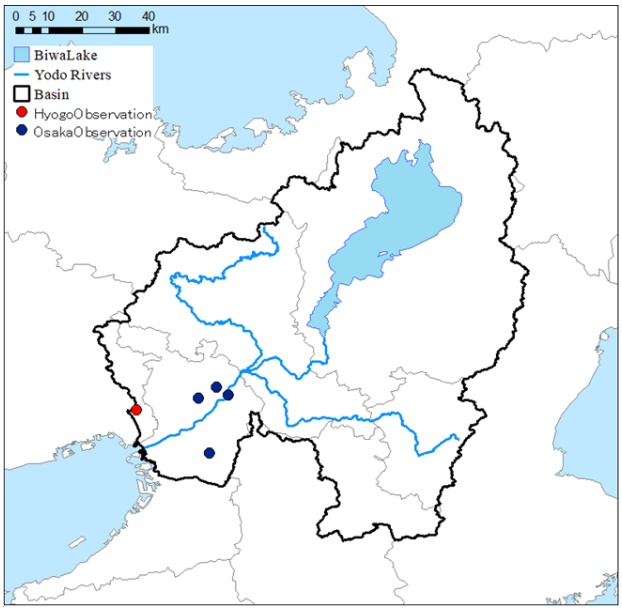

Figure 16. The location of Pb observations.

Figure 15(a) shows the spatial distribution of annual atmospheric concentration every 12 years from 1956 to 2016. The concentration distribution in the atmosphere is mainly affected by the emission amount. It can also be seen that the concentration variation was particularly large in the downstream area of the Yodo River, where there are large quantities of pollution sources such as buildings, roads, and industrial establishments.

3.4.3 Pb in soil

It can be seen that the concentration gradually increased from 1957 to 2007 and became stable after 2007 (Figure 13). The concentration in the soil media increased rapidly, particularly between 1957 and 1969. The concentration fluctuation was large compared to other years because the amount of deposition from the atmosphere was higher than that in other years. However, the speed of increase rapidly decreased in 1975 due to a sudden decrease in deposition from the atmosphere.

The distribution of the annual concentration of Pb in the soil media every 12 years is shown in Figure 15(b). It was also found that the areas where the concentration continued to increase gradually decreased. The concentration in the lower reaches of the Yodo River was the highest, followed by the southern part of Lake Biwa. This is because the Pb emissions from road marking paints around the expressway and the national highway in the southern part of Lake Biwa were substantial.

3.4.4 Pb in water

Figure 13 also indicates that the annual concentration in the entire basin in the water body showed a slightly increasing tendency. During the entire simulation period, the concentration increased, while the rate of increase gradually decelerated. Moreover, the concentration decreased slightly in 1970, 1975, and 1978 owing to a decrease in Pb discharge. Figure 15(c) shows the distribution of Pb concentrations in water every 12

years during the study period. It can be indicated that the high concentration area was found in the southern part of Lake Biwa and the concentration in the lower reaches of the Yodo River was the highest. The Pb from the road marking paint was discharged directly into the water, and the Pb in the soil media flowed into the water by rainfall. However, the area where the Yodo River passes shows a low concentration because the quantity of water is too large to dilute the Pb concentration. It was also found that the Pb accumulation in the southern part of Lake Biwa was markedly faster than in other places, which may cause environmental risks.

3.4.5 Pb in sediment

According to Figure 13, similar to the results for the water body, the Pb concentration of the entire basin in the sediment media gradually increased during the simulation period. Figure 15(d) shows the special distribution of concentration in the sediment media every 12 years. The concentration in the lower reaches of the Yodo River in the southern part of the basin was considerably higher than that in other locations. However, unlike the water media, the area where the Yodo River passes also showed a high concentration. In addition, the area around Lake Biwa, where rivers cross, was expressed at high concentrations. This was because the sedimentation from water in these areas was larger than that in other places, therefore, Pb accumulation was severe.

3.5 Conclusion

It is necessary to monitor the concentrations of hazardous chemicals emitted by human activities that affect human and ecosystem health. In this study, a distributional type multimedia model was developed based on a one-box type model for Pb. In the model, the study area was divided into tiny meshes, and each was divided into four environmental media: atmosphere, soil, water body, and sediment, similar to the one-box type model.

The model was applied to the Lake Biwa-Yodo River basin, and the calculation period was extended to 60 years from 1957 to 2016. The amount of Pb emissions in the basin was estimated and distributed into each mesh inside the basin. The validity of the distributional model was evaluated by comparing it with measured Pb concentrations.

The distributional multimedia model can predict the spatial distribution of harmful chemical concentrations, which a one-box type cannot predict. In the atmosphere, the spatial average Pb concentration simulated by the distributional type model was close to the one-box model results, however, both were lower than the observations. The reason for this underestimation was the simplification made in the model, including the emission estimation and boundary condition of the target area. However, a portion of the study area showed higher concentrations than those of other places, which should be warned of potential environmental risks. In soil and water media, the distributional model indicated that high-level Pb concentrations occurred in the lower reaches of the Yodo River. The main reason for this was the emissions discharged due to heavy human activities. The large population in these areas should be warned of the potential environmental risk of a high Pb concentration.

4 Apply to mercury

4.1 Introduction

Mercury (Hg) is a major toxic metal, which has been widely used from ancient ages. Cinnabar, which contains mercury sulfide (HgS), has been used in Chinese traditional medicines for thousands of years (Liu et al., 2008). Moreover, Cinnabar-based paint was also used to color Egyptian tombs and Shang ruins in China. In modern life, Hg is still a common material used in the industry. Further, Hg can be found near our body, such as thermometers and fluorescent lamps.

The human body can easily absorb Hg which are widely distributed in the environmental media and circulate by vaporization and precipitation between air, soil and water. Hg can roughly divide into three chemical forms: metallic mercury, inorganic mercury, and organic mercury. Metallic mercury (Hg0) is liquid at room temperature and is easy to vaporize which has been used for clinical equipment such as thermometers. Metallic mercury vapor can be absorbed into human body through the lung while breath. One of the organic mercuries, the Methylmercury ($MeHg^+$) is naturally generated from inorganic mercury by bacteria in the water environment which can be accumulated in fish and mammals through the food chain. By eating them, Methylmercury can enter the human body through the intestinal tract. The inorganic mercury includes such as mercuric (II) oxide, mercuric (II) sulfide, etc. These Hg (II) compounds have high deposition velocities and are more easily methylated than elemental Hg when then enter ecosystems (Hu et al., 2013). 1400 tons of Hg from tailings and vaporization are released each year, and between 10 and 19 million people from over 70 countries are still using Hg in artisanal and small-scale gold mining (Esdaile and Chalker, 2018). Due to its chemical property and toxicity,

Hg is requested under longtime monitoring and risk assessment. The well-known Minamata disaster happened in 1956, until 12 years after the Japanese government indicated that the reason was Hg. Affected by the incident, the United Nations Environment Programme (UNEP) launched activities related to global mercury pollution in 2001. Members of the scientific community have played a critical role in the establishment of the Minamata Convention on Mercury (MCM), which is entered into force in August 2017, focusing on protecting human health and the environment from anthropogenic emissions and releases of Hg. Scholars continue to make more and more studies on the occurrence of Hg in the world. The distributional multimedia model has been developed and utilized to the Lake Biwa-Yodo River basin as one of approaches.

4.2 Methodology

4.2.1 Modifications

Based on the main structure of multimedia model, the application in Hg was modified due to the chemical characters. Figure 17 shows the detailed structure of the model.

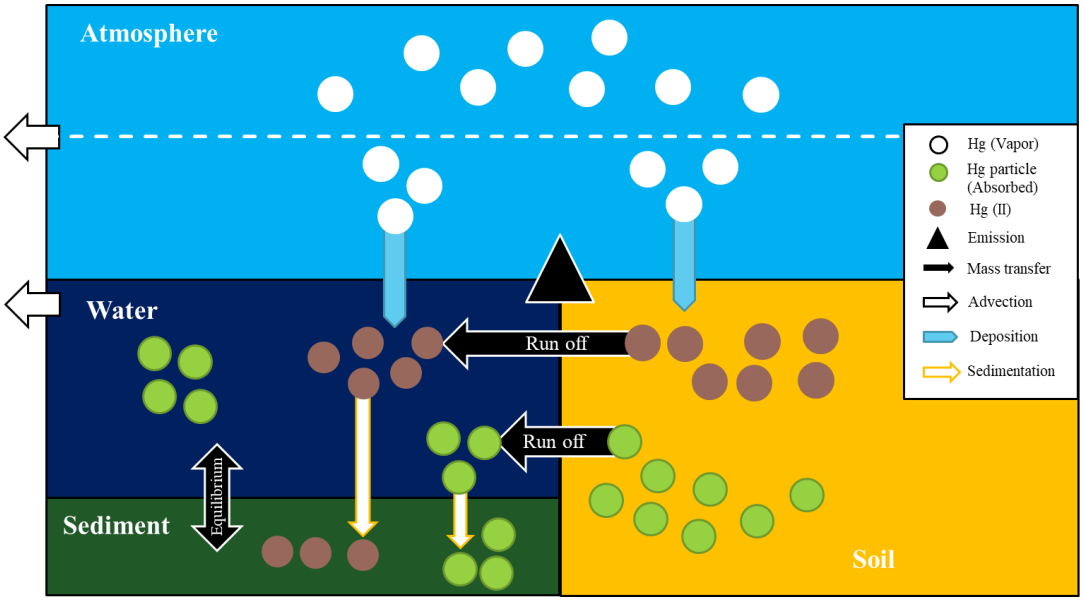

Figure 17. Structure of the distributional multimedia model.

In contrast to the one-box multimedia model, the distributional multimedia model divides the study area into numerous tiny meshes (Figure 1) instead of a single imaginary box. The total number of meshes in the Lake Biwa-Yodo River Basin was 8775, including 428 boundary meshes. Each mesh was constructed as a space with width, length, and height of 1 km, 1 km, and 2 km, respectively, and was labeled with the order of horizontal (west-east) and vertical (north-south) axes. The space inside one unit was separated into four environmental media: atmosphere, soil, water, and sediment, and the concentration of one substance was not distributed inside each medium. The atmospheric media consisted of two layers, the upper and lower atmosphere, and the thickness of the lower atmosphere (equivalent to the mixed layer) varied hourly in height from 200 – 1000m. The other media consisted of liquid and particulate phases (suspended solid phase in water). The thicknesses of the soil and sediment media were kept constant.

Mass exchange processes between environmental media include emissions, deposition, advection, and sedimentation. The details of these mass exchanges between the four environmental media are similar to those in the one-box multimedia model. Mercury emissions occur in the lower atmosphere, soil, and water bodies. Particles in the atmosphere deposit into water bodies and soil owing to gravity and rainfall. Suspended solids settle in the sediment medium. Owing to rainfall, some particles in the soil runoff into water bodies, and these particles become part of the suspended solids phase. For the soil, water, and sediment media, there is a cation exchange equilibrium between the particle and liquid phases. The advection processes in the atmosphere and water were considered. There were inflows from or outflows to neighboring meshes.

4.2.2 Equation and variables

Because the chemical form of Hg changes in different media, a total of eight sub-media

of each unit mesh were present in the distributional multimedia model (Table 2).

Table2. Sub-media in distributional multimedia model

Sub-media No.	Environmental media	Chemical forms
1	Atmosphere	Divalent mercury (Hg2+).
2		Gaseous metallic mercury (Hg).
3	Soil	Divalent mercury (Hg2+) (Liquid phase).
4		Absorbed mercury ions (Particle phase).
5	Water	Divalent mercury (Hg2+) (Liquid phase).
6		Absorbed mercury ions (Suspended solids).
7	Sediment	Divalent mercury (Hg2+) (Liquid phase).
8		Absorbed mercury ions (Particle phase).

The amount of Hg in each sub-media was calculated using the equation:

$$\frac{dM_i}{dt} = f_{e\_i} + \sum_{j=1}^{8} f_{eq\_ij} + \sum_{j=1}^{8} f_{dp\_ij} + f_{ad\_i} \quad (5)$$

where i and j are the order numbers, M is the molar amount, f_{e_i} is the emission flux, f_{eq_ij} is the mass transfer flux between media i and j due to equilibrium, f_{dp_ij} is the deposition and runoff flux from media i to j, and f_{ad_i} is the advection flux in media i affected by other meshes.

Beside the mass transfer inside each mesh, the affection from adjacent meshes were also considered in the distributional type model. Modifications are shown in the following.

- Exchange of Hg particles and ions between/in environmental media.

  Because the study area was divided into serials of unit mesh, material exchange between different media (inter media exchanges) were separated and labeled with x (west-east direction) and y (north-south direction). In detail, each variable was represented by a two-dimensional array.

- The mass transfer in the atmosphere by adjacent meshes.

  Hg concentration in atmosphere of each mesh were affected by meteorological phenomenon (wind) from adjacent meshes in four directions (north, east, south and west).

- The mass transfer in the water by adjacent meshes.

  Hg concentration in water of each mesh were affected by the water flow. The water flow was affected by the waterfall line, determined by the terrain height and river

direction if there was a river across that mesh geographically.

- The distribution of total mercury emission.

  There is a distribution of emission in each mesh and the amount were estimated separately.

Considering above modifications, the eight main variables describe the total mass of Hg in each media was reconstructed using two-dimensional arrays. Each variable was expanded into two-dimensional array and the subscript [x, y] means the west-east order of mesh is x, and the north-south order is y. After inter media exchanges, the mass transfer between neighbor meshes occurred. Table 3 shows eight modified variables used in the distributional multimedia model.

Table3. Main variables in distributional multimedia model

Variables	**Comments**
M2	Total amount of divalent mercury (Hg2+) in atmosphere.
Ma	Total amount of gaseous metallic mercury (Hg) in atmosphere.
M2sl	Total amount of divalent mercury (Hg2+) in soil liquid phase.
Mabssl	Total amount of mercury ions adsorbed in soil particle phase.
M2wt	Total amount of divalent mercury (Hg2+) in water liquid phase.
Msswt	Total amount of mercury ions adsorbed on SS in water particle phase.
M2sd	Total amount of divalent mercury (Hg2+) in sediment liquid phase.
Mabssd	Total amount of adsorbed ions in sediment particle phase.

4.2.3 Ion concentration variation

Since the substance to be calculated is a metal, dissolution equilibrium and ion exchange were considered in this study. In this section, the dissolution rate equation for calculating dissolution equilibrium and the amount of ion exchange that occurs on the surface of mineral particles were described in detail.

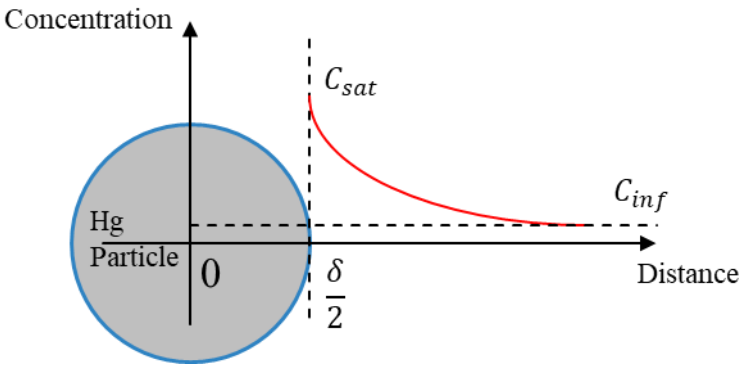

Figure 18 shows a conceptual diagram of exchange equilibrium.

- Dissolution rate

In soil, water, and sediment media, dissolution of Hg compounds into the liquid phase slightly occurred. Therefore, we consider the dissolution rate of Hg when they are present in water. A schematic diagram of dissolution is shown in Figure 18. The Hg concentration at the particle surface is the saturation concentration, and is the aqueous phase concentration at infinity, between which the compound moves by molecular diffusion. The dissolution rate J [mol/s/particle] from a single particle is expressed by equation:

$$J = 2\pi\delta D\left(C_{wtsat} - C_{inf}\right) \qquad (6)$$

where δ is the diameter of the particle; D is the molecular diffusion coefficient; C_{wtsat} is saturated solubility of Hg in water; C_{inf} is concentration of Hg in the liquid phase.

If the Hg total amount in the particle phase is M [mol], the total number of particles N can be expressed by equation:

$$N = \frac{6\times10^{-3}mM}{\delta^3\rho} \qquad (7)$$

where M is the total amount of Hg in the particle; m is the atomic mass of Hg; ρ is the density of the particle.

According to equation (5 – 6), the dissolution rate of Hg, K can be expressed by

equation:

$$K = JN = \frac{12\times10^{-3}\pi mMD(C_{wtsat}-C_{inf})}{\delta^2\rho} \qquad (7)$$

- Icon exchange equilibrium

  Hg deposited in soil is divalent cations. In soil, water, and sediment media, some of Hg ions in the liquid phase, are adsorbed on mineral particle surface through exchange equilibrium. The ratio of Hg ion concentration absorbed in particle phase (CHgS) and Hg ion concentration in liquid phase (CHgL) was the equilibrium coefficient of Hg ion. In this study, calcium ion (Ca+) was chosen as a representative of ions present in large amounts in the environmental media. The concentration of Ca+ in liquid phase CCaL and the concentration in particle phase CCaS were assumed to remain unchanged. And it was assumed that the equilibrium coefficient of Hg was proportional to the equilibrium coefficient of Ca+, which is the ratio of CCaL and CCaS. The above assumption is expressed by equation:

$$\frac{C_{HgS}}{C_{HgL}} = S\frac{C_{CaS}}{C_{CaL}} \qquad (8)$$

  where *S* is a scaling factor assumed in this study.

4.3 Emission estimation

This section describes the method of Hg emission estimation for different environmental media (air, soil, and water) from 1957 to 2009 in the Lake Biwa-Yodo River Basin. Although the most common uses of Hg worldwide are artisanal and small-scale gold mining (Esdaile and Chalker, 2018), such mining is absent at present in Japan, and only recycled and imported Hg is currently used. Until the 1990s, Japan still used large quantities of Hg. Subsequently, Hg consumption declined and was limited to fluorescent tubes and measuring instruments. The emissions estimation was roughly divided into

several time periods using different methods and data sources.

4.3.1 Hg emissions before the 1990s

Mercury has been used in large quantities for the chlor-alkali industry, catalysts, inorganic chemicals, pesticides, measuring instruments, and vinyl chloride production. Because there were no direct data on historical emissions, Hg emissions before the 1990s were estimated based on industry Hg usage. The usage of Hg were published by the National Institute for Environmental Studies at a public seminar on Hg (Akiko Kida, 2012). The national Hg consumption for the most common uses in Japan from 1957 to 1990 was shown in Figure 19.

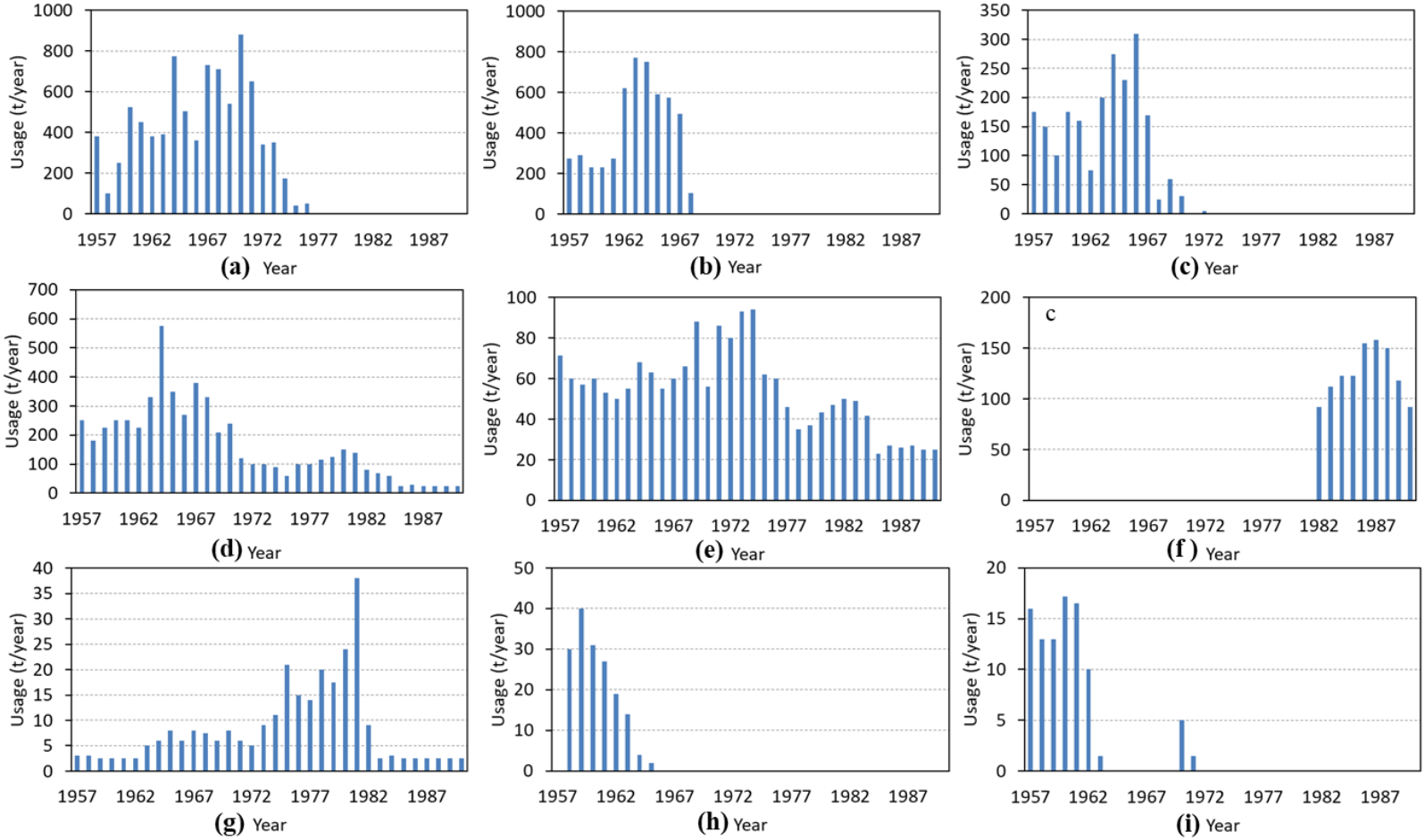

a) chlor-alkali industry; b) catalyst industry; c) pesticide industry; d) inorganic chemical industry;
e) measuring instruments; f) batteries; g) medical products and amalgams; h) gunpower; i) paints;

Figure 19. Hg consumption in different industries from 1957 to 1990.

In the present study, 10% of the Hg consumed in the chlor-alkali and catalyst industries was assumed to be disposed into water and exposed to the environment. The amount of Hg adhered to crops is reported as approximately 1/3 of the total amount sprayed on paddy soils (Nakagawa et al., 1991). Therefore, the current study assumed that 2/3 of the 880,000 tons of Hg-containing pesticides used in Japan were deposited in soil and thus regarded as emissions. Mercury consumption by other industries was assumed to be incinerated and discharged into the environment at the time of product disposal. Mercury emissions inside the Lake Biwa-Yodo River Basin were proportional to the basin's population.

4.3.2 Hg emissions after the 1990s

After the 1990s, reliable Hg emission data were obtained from the Pollutant Release and Transfer Register (PRTR) system, which is a chemical management policy established by the Japanese government. The PRTR system requires business operators to submit notifications to regional or municipal governmental authorities regarding specified chemical substances that may be harmful to human health and ecosystems. The data from the PRTR system include the nationwide amounts of chemicals released into the air, water, and soil available to the public. There were two types of Hg emission data: reported and unreported. The reported part includes Hg emissions from business operators who need to report to the local government once a year, whereas the unreported part includes emissions from those who are not required to report such data. The PRTR system calculates the total reported emissions and estimates the amount of unreported emissions using its own method (Ministry of Economy Trade and Industry).

However, the PRTR system has been in effect only since April 2001, and Hg emissions data are lacking before 2001. Thus, both reported Hg emissions and unreported emissions

for 1991–2000 were complemented using linear interpolation.

4.3.3 Hg emission to each media

The historical emissions from 1957 to 2009, estimated using the above methods, are shown in Figure 20.

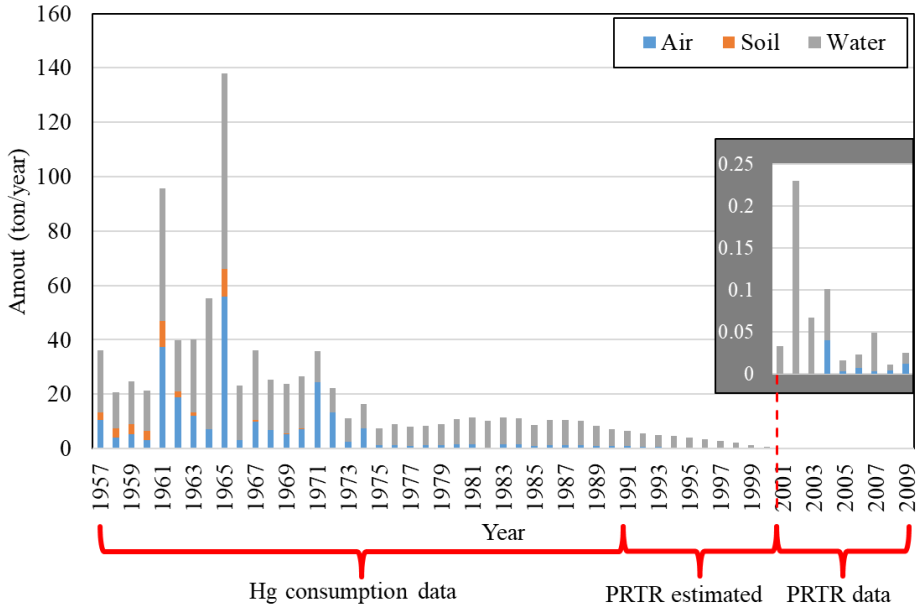

Figure 20. Annual Hg emission to different environmental media.

4.3.4 Hg emission distribution

The distribution of total emissions to each mesh was based on the Industrial Statistics Survey (Ministry of Economy Trade and Industry) and the National Land Information (Ministry of Land Infrastructure Transport and Tourism). The Industrial Statistics Survey lists the number of business establishments, employees, and product shipments by industry sector for all municipalities (cities, towns, and villages) in Japan, which were mainly used in this study. The National Land Information system was developed to assist in the formulation and implementation of national land planning. The data consists of classifications (paddy fields, orchards, forests, lakes, rivers, waste areas, building areas, and transportation areas) and area sizes in tertiary mesh units based on the status of

nationwide land usage.

The method of distributing Hg emissions into every divided mesh was calculated differently, depending on the emission source. In the PRTR system, every business operator's establishment distributed the reported emissions to the mesh where they were located. The unreported emissions of one municipality were allocated to all meshes belonging to that municipality in proportion to the population. Emissions estimated for consumption by different industries (such as chlor-alkali, catalysts, and pesticides industries) in each prefecture were summed and then distributed equally to all meshes that were classified as industrial areas. Other Hg emissions were distributed across all meshes in proportion to the mesh population. The distribution of emissions to air, soil, and water, with the highest value in 1965, was shown in Figure 21.

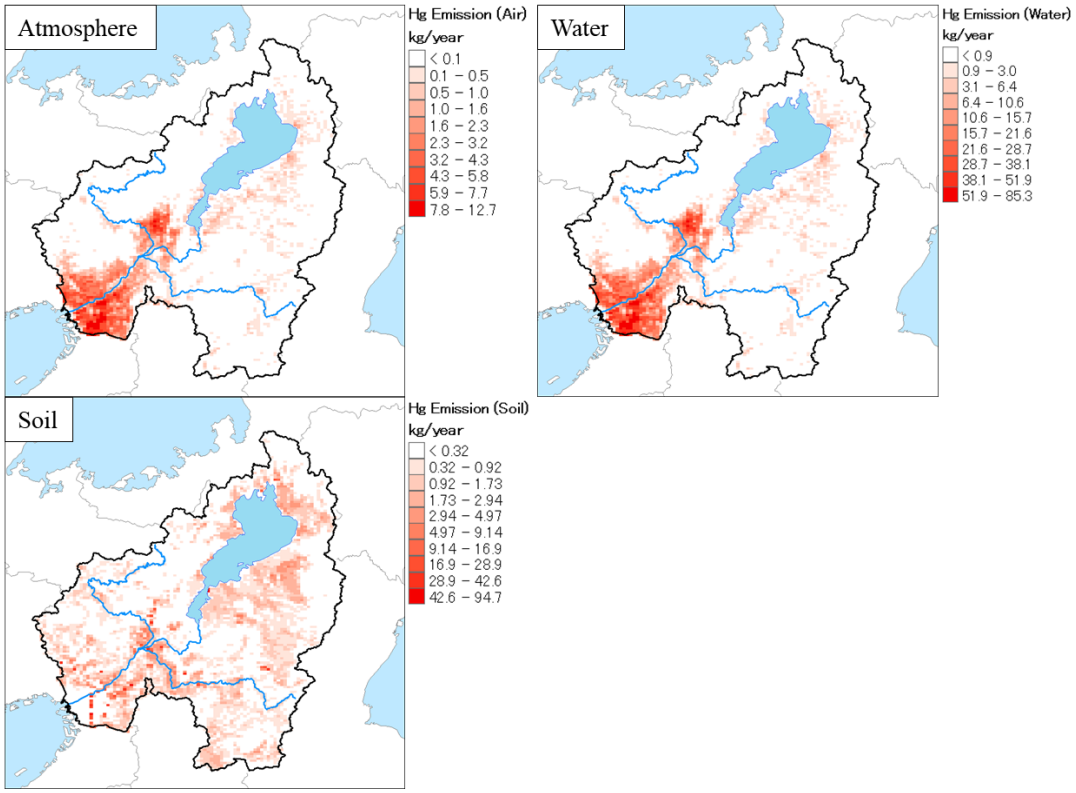

Figure 21. Distribution of Hg emission in 1965.

4.3.5 Hg emission from outside the basin

Most Hg emitted into the atmosphere by human activities is gaseous metallic Hg, which moves with the atmosphere and affects areas far from the source of emissions. Therefore, it is necessary to consider long-range atmospheric transport in terms of influent air outside the Lake Biwa-Yodo River Basin. Because Asian anthropogenic emissions of Hg to the atmosphere contribute 54% of all anthropogenic emissions (Jaffe and Strode, 2008) and China is the largest emitter of anthropogenic Hg worldwide (Zhang et al., 2015), the Hg concentration of the influent air was assumed to be proportional to the gross domestic product (GDP) of China. In this study, the Hg concentrations measured in Okinawa (close enough to China) in 2007 were assumed to be the concentrations of the influent air (Ministry of the Environment). This study assumed that the historical Hg concentrations in other years were proportional to the GDP of China. Figure 22 shows the Hg concentration in the influent air entering the basin.

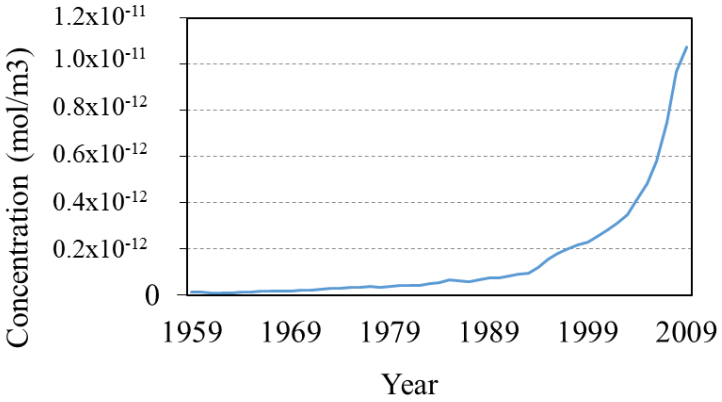

Figure 22. Hg concentration of influent air.

4.4 Result

The concentration of Hg in the Lake Biwa-Yodo River Basin was simulated for each year from 1959 to 2009 using the distributional multimedia model. The calculated concentration was compared with the measured data, including the Hg concentration in air and sediment published by the government (Osaka Prefecture Government). Figure

23 shows the annual Hg concentration in each medium of the Lake Biwa-Yodo River Basin, which was the value on the last day of the year from 1959 to 2009. The Hg concentration in the atmosphere fluctuated in the early years and showed a decreasing trend before 1975 owing to the relevant Hg consumption restrictions imposed in Japan. However, it showed a tendency to increase from 1975 in the atmosphere because of the increasing Hg concentration in the inflow air from outside the basin. Cross-border pollution from China may have contributed the most to this trend. This also indicates that the Hg concentration in the water body significantly decreased. The soil and sediment media showed a slight increasing tendency, indicating that Hg accumulated without migration. However, along with a reduction in emissions, the Hg concentration tended to a constant value.

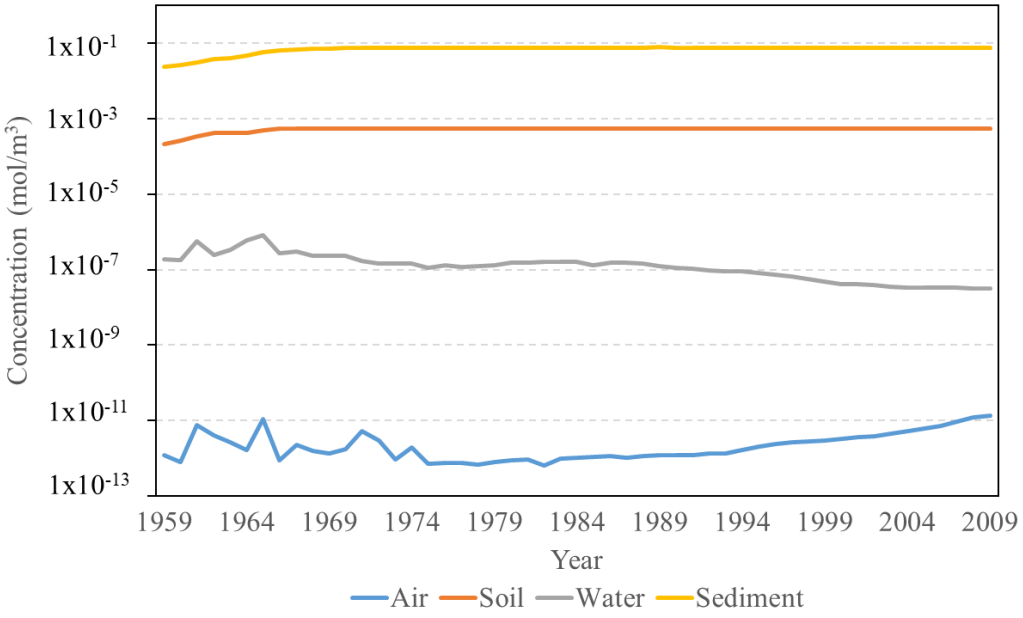

Figure 23. Annual Hg concentration from 1959 to 2009.

4.4.1 Comparison with observations

To evaluate the validity of the model, a comparison was made between the observed sites and the results of the simulation in year 2009. The locations of the observation sites are

shown in Figure 25. However, in the water media, as there were no measured values inside the Lake Biwa-Yodo River Basin, we compared the observed Hg concentrations in surface seawater around Japan in 2010 (Japan Meteorological Agency) instead of that. Figure 24 shows the measured Hg concentration of these locations compared with the annual concentration. In general, the calculated values in some environmental media (air, water, and soil) basically fit the observational values, whereas the Hg concentration in the sediment media was overestimated. Because the model structure assumed that sediment media was the final destination for Hg. In reality, some of the sediments were resuspended into the river body and run out of the study area. The simplification of runoff in sediment media might cause the overestimation.

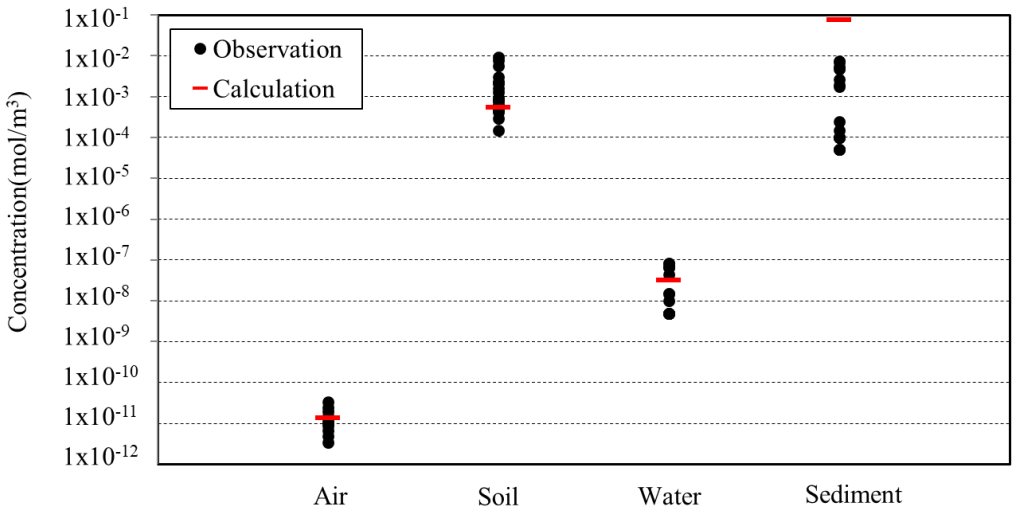

Figure 24. Comparison between simulation results and observations in 2009.

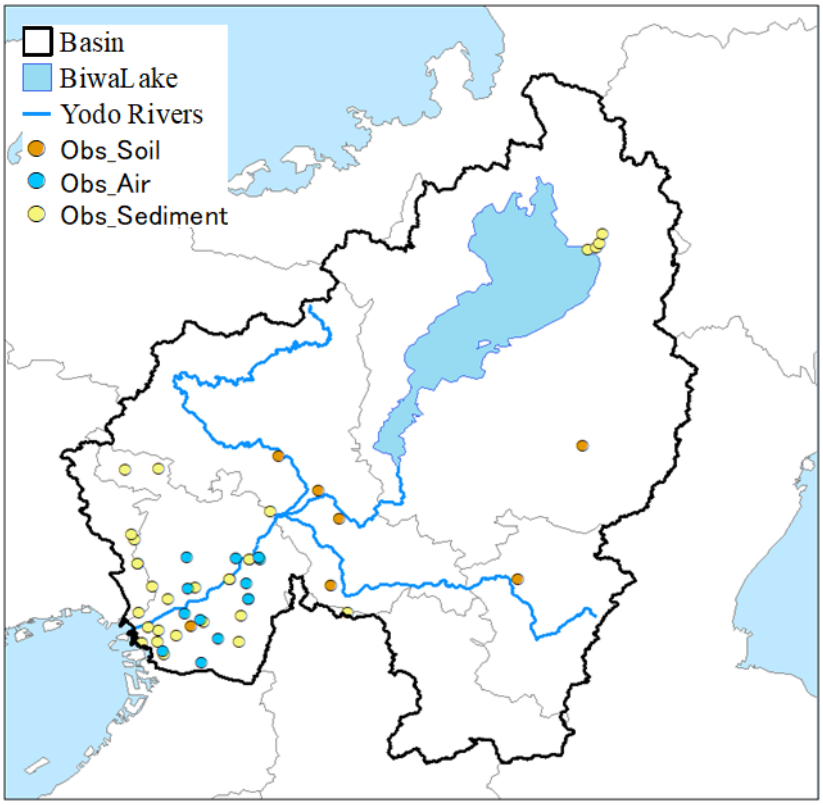

Figure 25. Hg observation sites in Lake Biwa-Yodo River basin.

To determine the accuracy of the model, this study also compared observed value and simulated result of every single mesh. A detailed comparison with the simulated concentration of those observation sites was shown in Figure 26. For water media, no comparison was made owing to the lack of observational data. In general, for such small area, the simulated results were close to the measured Hg concentration. In the atmosphere media, the calculated Hg concentrations in these locations tended to be overestimates, and those in soil media were slightly underestimated. In the sediment media, the calculation generally reproduced the observations, though some calculated values tended to be overestimated by two orders of magnitude, whereas some errors were within one order of magnitude or even less.

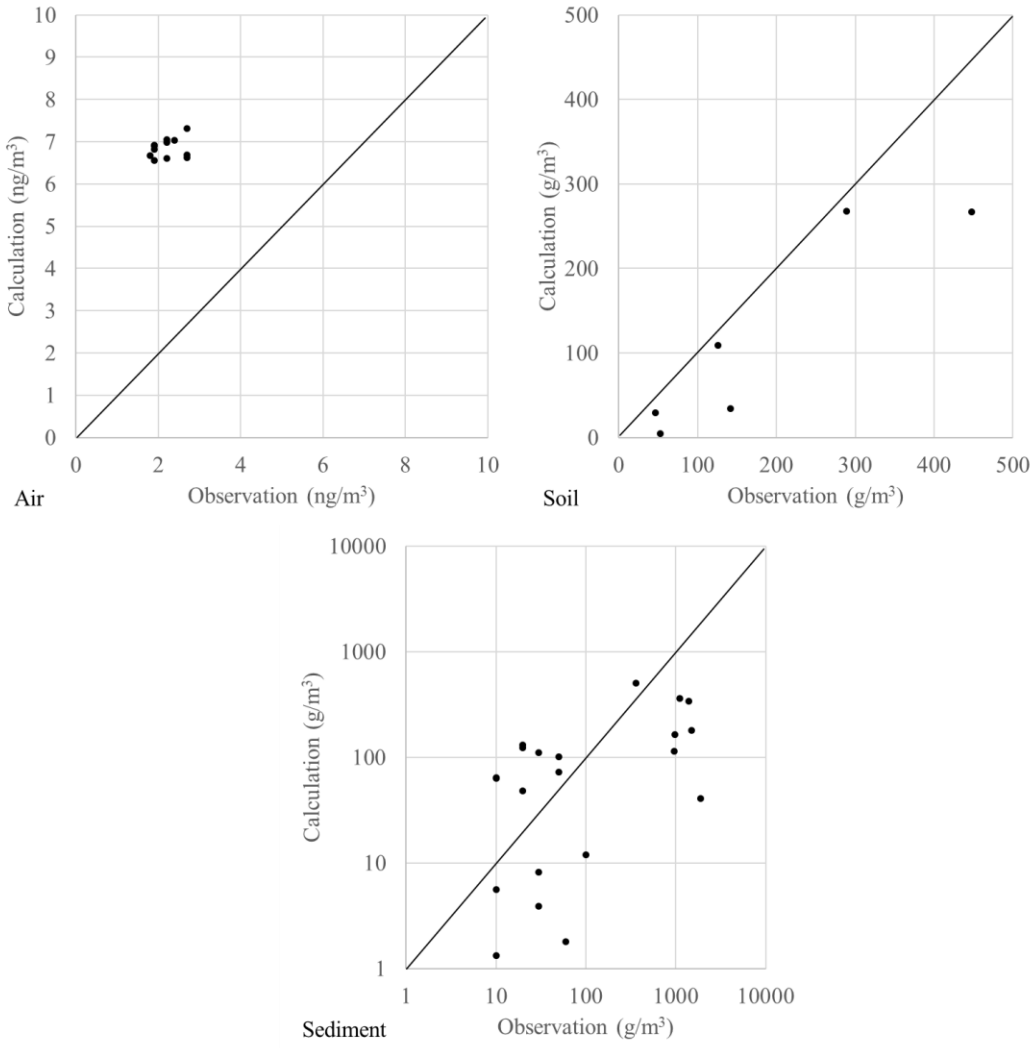

Figure 26. Comparison of calculated and measured values (2009).

The overestimation in air media might because the Hg concentration in the influent air entering the basin was overestimated. The estimation process in Chapter 4.5 has an uncertainty. The error might be acceptable due to its magnitude. In sediment media, the error was different to the other media. One possible reason is that the Hg concentration is highly related to the liquid-solid distribution coefficient. And in the present study, the liquid-solid distribution coefficient was assumed to be a constant value. Each location should have its own coefficient value, depending on the sediment composition and particle size. However, in spite of these errors caused by the simplification, the model still

has the ability to reproduce the real Hg concentration.

4.4.2 Distribution in the atmosphere

The distribution of Hg in the air at the end of 1959, 1969, 1979, 1989, 1999, and 2009, when emissions changed significantly, is shown in Figure 23. According to the distribution, the Hg concentration was high around the urban sites and northwestern part of the Lake Biwa-Yodo River Basin. Mercury in the air was transported to the suburbs from urban areas through advection until 1969. After 1969, the Hg concentration decreased over the basin, with particularly large decreases in urban areas owing to the decrease in Hg emissions. However, the Hg concentration in transboundary inflow air from China increased after 1979, although the concentration did not increase. This was because the deposition might carry most of the Hg into the water and soil.

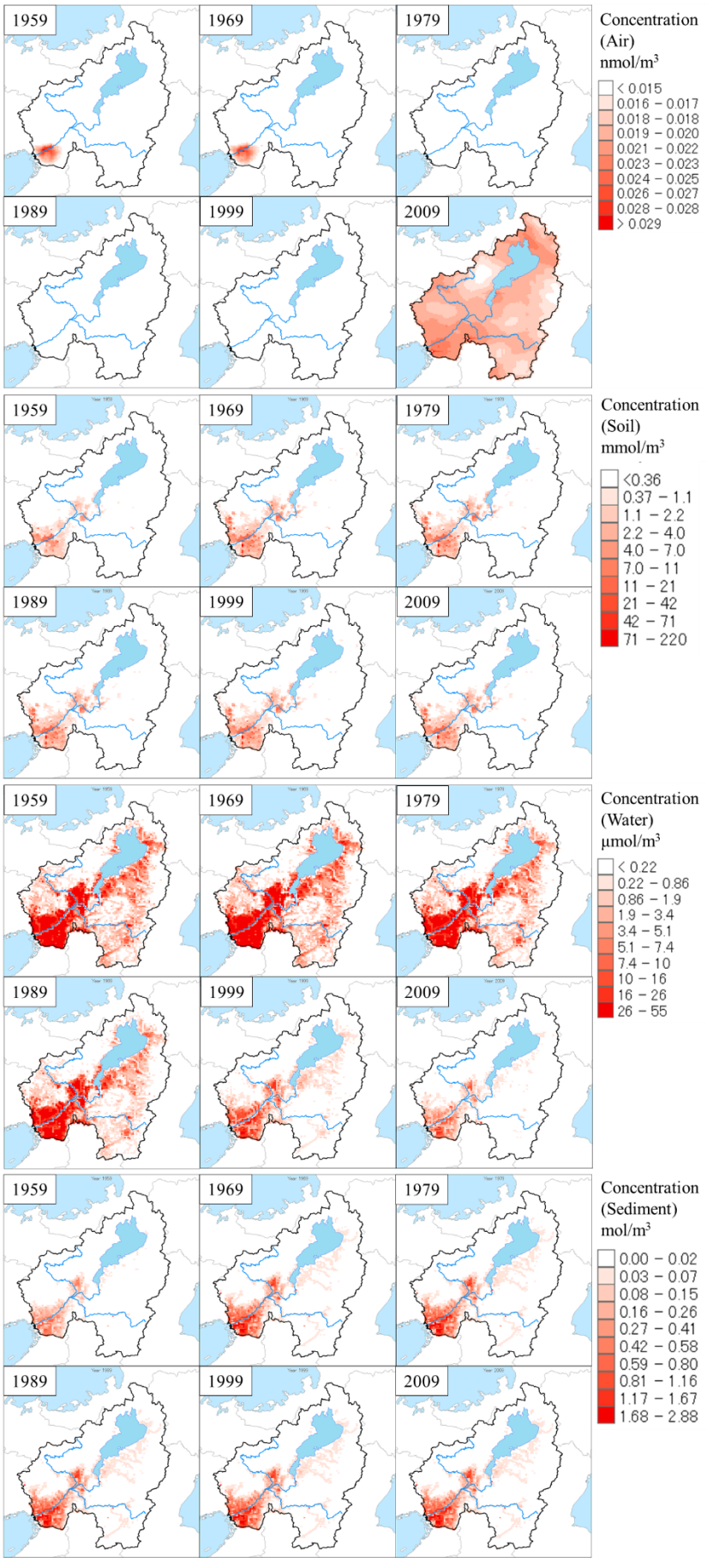
1959
1969
1979
1989
1999
2009
Concentration (Air) nmol/m³
< 0.015
0.016 – 0.017
0.018 – 0.018
0.019 – 0.020
0.021 – 0.022
0.023 – 0.023
0.024 – 0.025
0.026 – 0.027
0.028 – 0.028
> 0.029
Concentration (Soil) mmol/m³
<0.36
0.37 – 1.1
1.1 – 2.2
2.2 – 4.0
4.0 – 7.0
7.0 – 11
11 – 21
21 – 42
42 – 71
71 – 220
Concentration (Water) µmol/m³
< 0.22
0.22 – 0.86
0.86 – 1.9
1.9 – 3.4
3.4 – 5.1
5.1 – 7.4
7.4 – 10
10 – 16
16 – 26
26 – 55
Concentration (Sediment) mol/m³
0.00 – 0.02
0.03 – 0.07
0.08 – 0.15
0.16 – 0.26
0.27 – 0.41
0.42 – 0.58
0.59 – 0.80
0.81 – 1.16
1.17 – 1.67
1.68 – 2.88

Figure 27. Distribution of Hg in different environmental media.

4.4.3 Distribution in the soil

The distribution of Hg in the soil at 10-year intervals (1959, 1969, 1979, 1989, 1999, and 2009), when emissions changed significantly, is shown in Figure 23. Mercury concentration in soil increased continuously from 1959 to 2009 owing to emissions into the soil. In addition, Figure 27 shows locations (especially in the lower reaches of the Yodo River and the eastern region of North Lake Biwa) where concentrations were high because of the high population and developed economy that used a considerable amount of Hg-containing substances. In soil media, most of the Hg is strongly retained in the soil; hence, there is no spatial migration, and most of the Hg accumulates in the space where it is emitted. Although Hg emission to the soil in the urban areas was low, the concentration increased owing to atmospheric deposition, where Hg discharge was still largely affected by transboundary inflow air from China.

4.4.4 Distribution in the water

Figure 27 shows the distribution of Hg concentrations in water at 10-year intervals during the study period. A high concentration area was found in the southeast part of Lake Biwa and in the lower reaches of the Yodo River. There was also no spatial migration, and most of the Hg accumulated in the space where it was emitted. Although Hg emission reduced after 1979, the concentration for the entire area continually increased owing to atmospheric deposition, which carries Hg into water. As the Hg concentration in the inflow air from China increased, Hg in the atmosphere was flushed into the water by rainfall.

4.4.5 Distribution in sediment

Figure 27 shows the spatial distribution of Hg concentration in the sediment media at 10-

year intervals. The concentrations in the lower reaches of the Yodo River (southwestern part of the basin) and southeast of Lake Biwa were much higher than those in other locations. However, unlike the water media, the area where the Yodo River passes also showed a high concentration. This was because the sedimentation from water in these areas was larger than that in other locations; therefore, the accumulation was severe.

4.5 Conclusion

In this part, sediments and soil media of the Lake Biwa-Yodo River Basin showed the accumulation of Hg in the long-term by using the distributional multimedia model. The calculated Hg concentrations no longer raised significantly and were becoming constant due to Japan successfully controlled the national usage of Hg except in atmosphere due to the effect of transboundary pollution. In terms of geographical distribution, for urban sites in the study area, the lower reaches of the Yodo River showed higher concentrations than other locations due to high Hg discharge from human activities. The distributional multimedia model could reproduce and predict the Hg concentrations in different media by comparing the calculated Hg concentrations with the observed Hg concentrations in four environmental media and in different place. Though the simulated values in the soil media were underestimated due to the parameter setting, the simulated Hg concentrations in other media were close to the observation. Moreover, the model could even reproduce the real Hg concentration for the small area around the observation point.

This study provides both special and temporal details of the environmental condition related with Hg. By using the distributional multimedia model, the simulation could calculate or predict the Hg concentration in specific areas. Also, by changing the input data including the emission, the developed model can be used for further studies to evaluate the geographical Hg occurrences in different environmental conditions.

Interested parties such as authorities responsible for environmental monitoring and management could use this study to develop environmental policies better. The model could be used to assess the environmental impacts under different emission permits (including the amount and the location of emission). Also, by fixing the pre-defined parameters of the model, modifying some assumptions and improving the simplification of mass exchange process of the model, the calculation errors can be eliminated, and the calculation results can be further improved. Furthermore, the approach of this study and the structure of multimedia model could provide inspersion for assessment of other pollutants, which can make the environmental monitoring process more successful.

5 Apply to sulfa drugs

5.1 Introduction

Chemicals which are the active substances of pharmaceutical and personal care products (PPCPs) have been detected in trace amounts from the environment (Sun et al., 2016; Tamura et al., 2017). Veterinary medicines, as one of the PPCPs, are used in large quantities on agriculture industry. There is an increasing concern about the ecological consequences of chronic exposure to the chemicals. Sulfa-drugs, which are typical antibiotics, are frequently found in the environment media, especially water bodies, such as river (Tamtam et al., 2008) and lake (Liu et al., 2018). When a sulfa-drug is used for human beings, the chemical substances contained therein are metabolized in the body, and then released into the sewage as a metabolite. Those left without being treated in the sewage treatment plant are released into the river. On the other hand, when a veterinary medicine is used for livestock, after metabolized in their body, the chemical substances are discharged as manure. Most of manure is reused in farmland after composting treatment and liquid fertilization treatment while some of the manures are not subject to carbonization or incineration or wastewater purification treatment and even discharge to the environment directly such as field piling or digging. This study focuses on sulfa-drugs and chooses 2 substances which belong to sulfonamide type synthetic antibacterial agents, and are sold in large quantities among veterinary drugs.

5.2 Methodology

5.2.1 Modifications of model

In this study, the kinetics of sulfa-drugs for livestock discharged into the environment were analyzed using the distributional multimedia models for the Lake Biwa-Yodo River

basin. According to the chemical properties of sulfa drugs, the mass transfers between four environmental media are shown in Figure 28. The substances movement caused by advection in the air and water media from the adjacent area is took into the consideration. The atmosphere media consists of gas phase and particle phase, and is divided into the upper layer and the lower layer corresponding to the mixed layer. The water media consists of liquid phase and suspended solid phase, and considers outflow from soil and equilibrium with sediment.

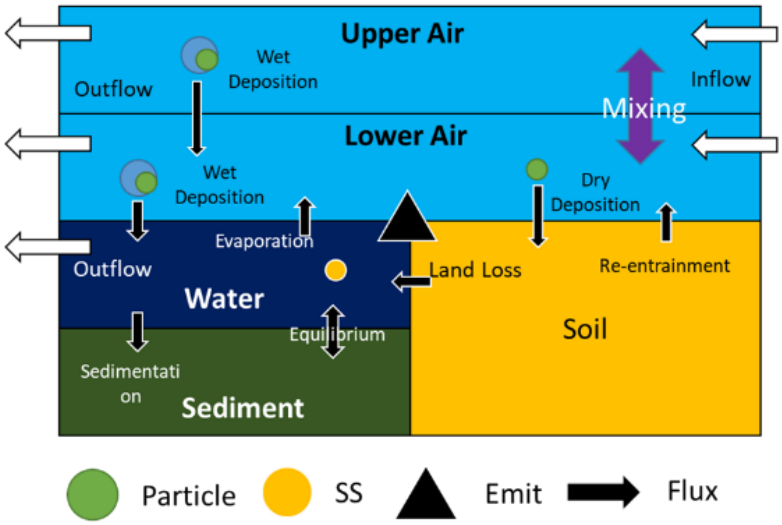

Figure 28 Structure of the Multimedia Model

Table 4. Main variables in distributional multimedia model

Variable	**Explination**
Mgsu	Total amount of gaseous state in the upper atmosphere
Mgsd	Total amount of gaseous state in the lower atmosphere
Mptu	Total amount of chemicals absorbed in particles in the upper air
Mptd	Total amount of chemicals absorbed in particles in the lower air
Msl	Total amount of chemicals in soil media
Mwt	Total amount of chemicals in water media
Mss	Total amount of chemicals absorbed in suspended solids
Msd	Total amount of chemicals in sediment media

5.3 Emission estimation

5.3.1 National emission

This study focused on two typical kinds of sulfa-drugs, sulfamethoxazole (SMX) and sulfadimethoxine (Albon) which are widely used in Japan as an antibacterial agent for livestock production. Since they are synthetic drugs which show persistent degradability in nature compared to drugs made of natural extracts, it is important to monitoring these two substances. According to statistical data by the Ministry of Agriculture, Forestry and Fisheries (MAFF), SMX is used in a larger amount than any other sulfur antimicrobial agents. Japan began statistics on veterinary drug sales since 2005 based on the promulgation of the MAFF Ordinance No. 62 Animal Medicines Regulation Rules. In this research, the amount of 2 chemicals that were released into the environment was estimated based on the national sales amount of pure active substance sulfa-drug (an example shown in table 5) from 2005-2015 (Tamtam et al., 2008).

Table 5. Sales amount (active substance) and proportion by animal in 2005

Year	Substance	Amount of pure active substance (kg)	Beef Cattle (%)	Dairy Cow (%)	Pig (%)	Broiler (%)	Layer (%)
2005	SMX	67723.1	0.0	0.0	89.4	7.4	3.3
	Albon	10810.7	9.8	5.4	40.1	32.9	7.8
2006	SMX	94260.3	0.0	0.0	93.0	4.6	2.4
	Albon	9127.2	3.5	3.7	47.0	34.0	11.5
2007	SMX	71045.2	0.0	0.0	91.9	5.4	2.7
	Albon	4534.1	11.2	8.0	44.5	22.5	15.0
2008	SMX	72135.1	0.0	0.0	94.0	1.6	4.4
	Albon	6570.6	8.3	6.7	40.6	32.4	12.8
2009	SMX	76246.4	0.0	0.0	91.2	3.4	5.4
	Albon	5072.0	10.5	8.8	43.7	26.6	10.8
2010	SMX	56552.4	0.0	0.0	97.5	1.4	1.1
	Albon	3474.3	8.7	15.8	23.3	44.0	9.1
2011	SMX	59586.9	0.0	0.0	89.1	4.3	6.6
	Albon	3164.5	9.0	16.1	30.4	37.5	7.2
2012	SMX	63724.0	0.0	0.0	88.0	5.7	6.3
	Albon	3018.0	9.5	17.4	45.4	14.6	8.5
2013	SMX	69050.9	0.0	0.0	87.0	6.0	7.0

	Albon	2231.5	10.8	19.3	48.2	11.5	3.2
2014	SMX	63141.3	0.0	0.0	77.3	18.0	4.7
	Albon	2580.4	11.6	17.4	46.0	8.8	10.5
2015	SMX	60223.7	0.0	0.0	79.7	16.1	4.2
	Albon	1628.1	13.8	18.6	47.1	7.7	5.7

5.3.2 Local emission

A sulfa-drug administered to domestic animals is eventually discharged outside their body as excrement after organ metabolism. In this study, it was assumed that all sulfa-drugs administered were finally excreted into the environment, there was no residual in livestock's organ and the usage of sulfa-drugs and excrement volume per livestock (same species) were uniform across the whole country. There was no difference in different place. The emission in a specific area was only affected by the animal amount. In other word, according to above assumption, the emission was only related to the excrement volume made by the animals.

Table 6. Excrement amount national and in different prefectures (unit: 1000 ton)

	Cattle	**Cow**	**Pig**	**Broiler**	**Layer**
National	23570	24420	22380	7450	5140
Mie	123	244	278	260	40
Shiga	56	168	12	18	5
Kyoto	108	64	26	85	28
Osaka	27	6	15	4	0
Hyogo	251	468	50	235	120
Nara	73	29	15	22	3
Sum	638	979	396	624	196

Based on the ratio of 6 prefectures (Osaka, Kyoto, Hyogo, Shiga, Mie, Nara) included in the Lake Biwa-Yodo River basin and national livestock excreta (Table 6) (Ministry of Agriculture Forestry and Fisheries; Liu et al., 2018), the sulfa-drug emission in the basin, E_{lcoal} were calculated by using the equation.

$$E_{local} = \sum_{i=0}^{n} E_{i,all} \cdot \frac{S_{i,local}}{S_{i,all}} \qquad (9)$$

where i is the type of animal, E_{all} is national sulfa-drug emission, S_{all} and S_{local} are livestock excreta in the nationwide and in the Lake Biwa-Yodo River basin, respectively.

Based on the data, the local (sum of 6 prefectures in the Lake Biwa and Yodo River Basin)

usage of 2 sulfa drugs (SMX and Albon) were showed in Table 7. In case, SMX is 253.279 g/mol and Albon is 310.33 g/mol. The total usage of 6 prefectures is only 2 – 3% of the national usage in Japan. The emission discharged to the environment were the same proportion according to the assumption. The annual emissions in different prefectures are shown in Figure 29.

Table 7. The national and local drug emission (unit: mol)

Year	SMX			Albon		
	National	Local	Rate	National	Local	Rate
2005	267652.8	6222.0	2.3%	33123.3	1419.5	4.3%
2006	372160.0	7926.0	2.1%	28640.3	1220.7	4.3%
2007	280501.7	6132.9	2.2%	14486.1	541.7	3.7%
2008	284804.9	5632.8	2.0%	20972.2	891.3	4.2%
2009	301037.2	6356.6	2.1%	16104.4	627.7	3.9%
2010	223281.0	4244.8	1.9%	10841.7	551.6	5.1%
2011	235261.9	5157.1	2.2%	9871.2	460.4	4.7%
2012	251596.1	5724.4	2.3%	9164.3	311.1	3.4%
2013	272627.8	6292.0	2.3%	6609.9	209.4	3.2%
2014	249295.4	7544.3	3.0%	7815.1	242.3	3.1%
2015	237776.1	6885.4	2.9%	4828.9	144.0	3.0%

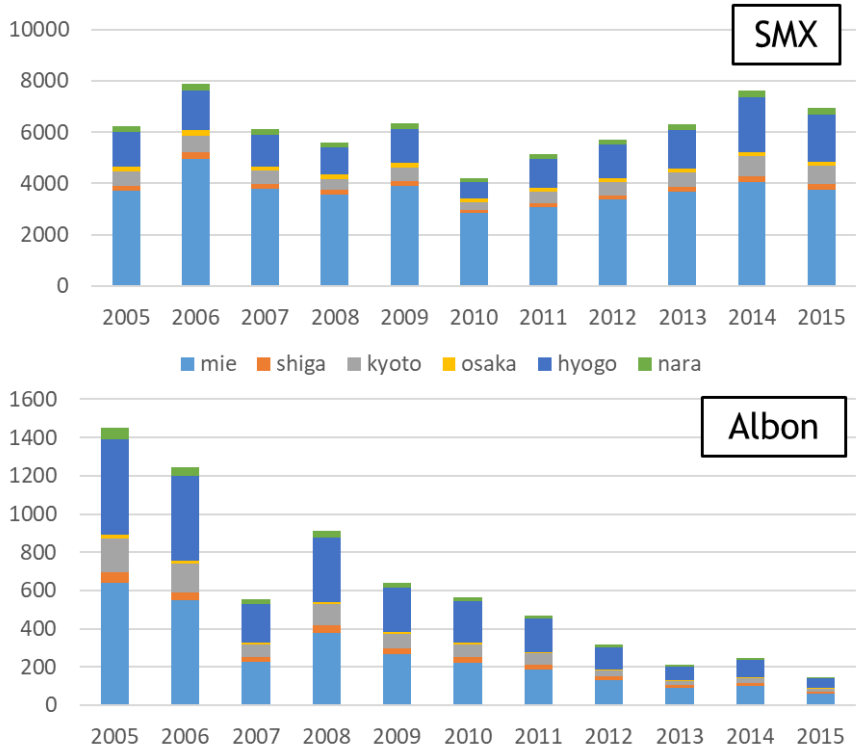

Figure 29. Estimated annual usage of sulfa-drug in 6 prefectures (unit: mol).

5.3.3 Emission distribution

The spatial distribution of sulfa-drug emission in the Lake Biwa-Yodo River basin was estimated by using the following equation, based on the farmland promotion (shown in Figure 30) according to the land use fragmented mesh data from the National Land Numerical Information System (Ministry of Land Infrastructure Transport and Tourism, 2022).

$$E_{mesh} = E_{all} \cdot P_{mesh} \quad (10)$$

The spatial distribution was shown in Figure 31. It can be indicated that most emissions of the sulfa-drugs were concentrated in the east and south of the Lake Biwa-Yodo River basin. In terms of the temporal trend, the Albon was decreasing while SMX was basically the same.

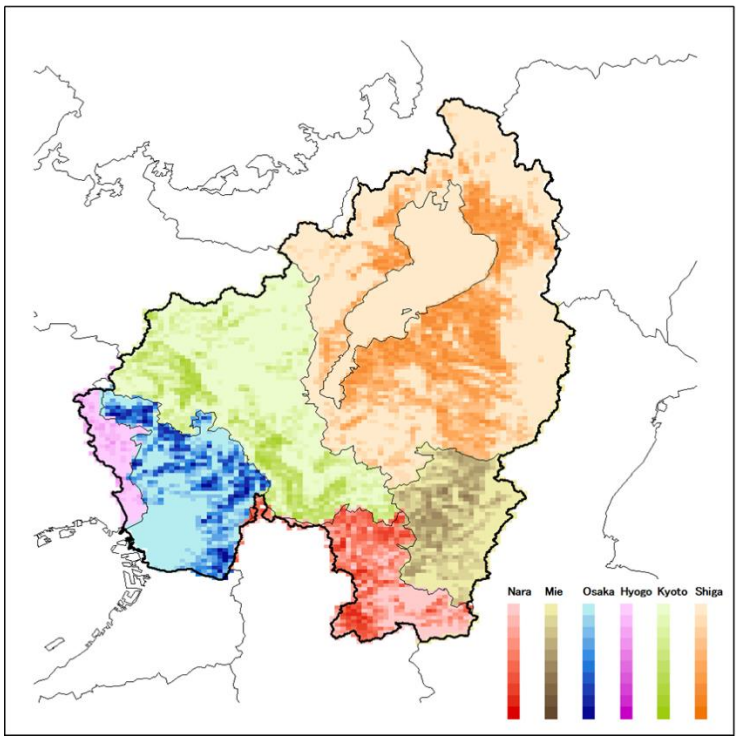

Figure 30. Farmland proportion of each mesh in different prefectures.

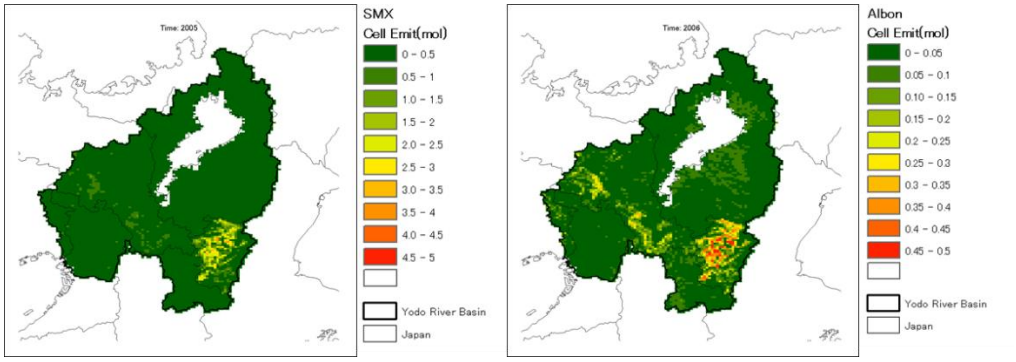

Figure 31. Emission distribution of SMX and Albon in 2006.

5.4 Result

5.4.1 Average annual concentration

As the result of the One Box Type multimedia model, the annual environmental amount of SMX and Albon was showed in the Figure 32, 33 respectively. The results of the residual and emission showed that, the environment residual of SMX was only 7.2% of that year's emission, while the Albon residual was 8.0% of the year. The annual concentration of the chemicals was basically related to the emission estimation. The trend of 2 kinds sulfa drug was almost the same as the emission. Albon was decreasing while SMX was waved in a small variation and was roughly equal.

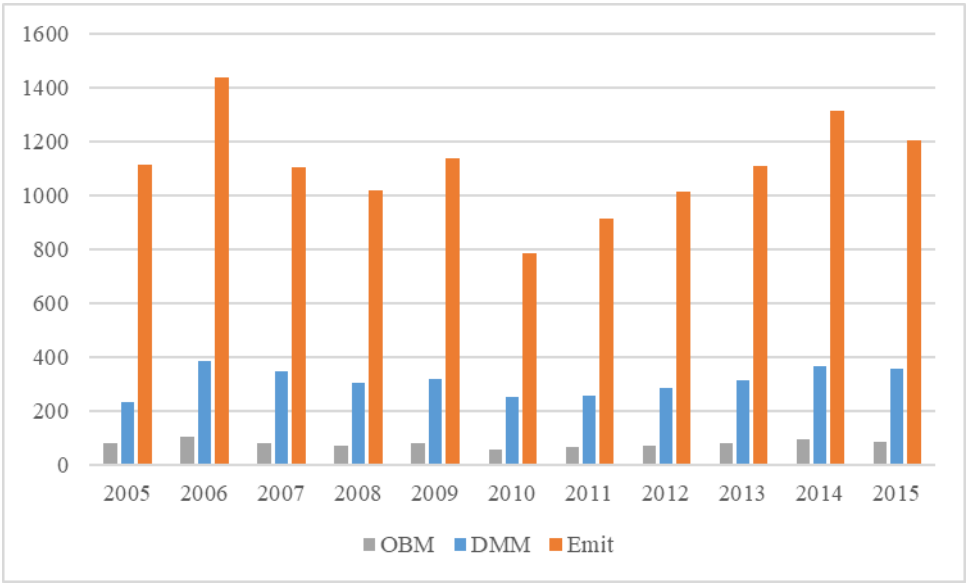

Figure 32. Amount of SMX emission and residual in environment.

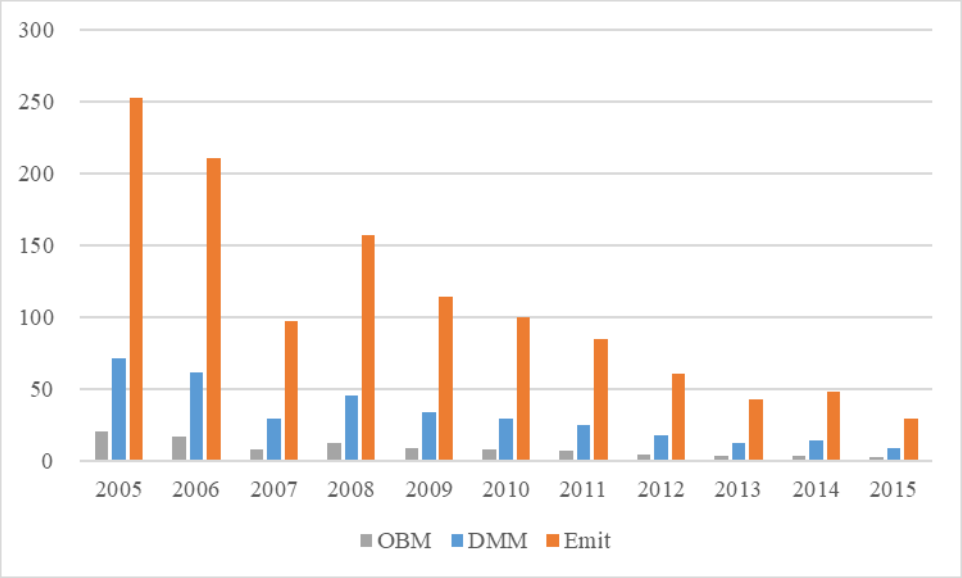

Figure 33. Amount of Albon emission and residual in environment.

The total amount of residual substances in each environmental medium is different. The proportion of SMX in different media was that, about 20% of the environmental residual is absorbed in soil, 79% of them are dissolved in water and there was no concentration in the atmosphere (either gas or particle) and suspended solids. The residual proportion of Albon was about 68% of the residual was dissolved in water and 30% was absorbed in soil. As the same, there were no concentration in the atmosphere and suspended solids.

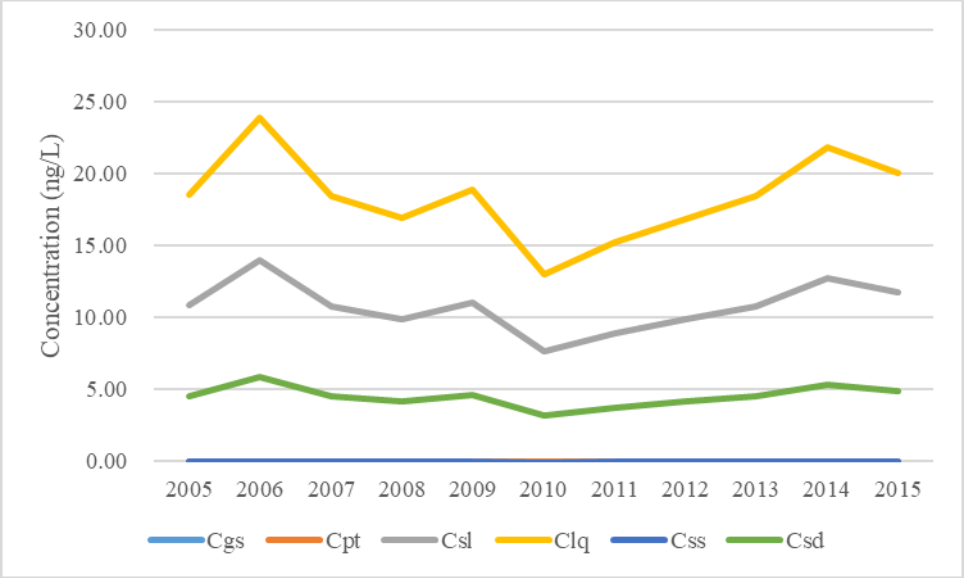

Figure 34. Concentration of SMX in each media.

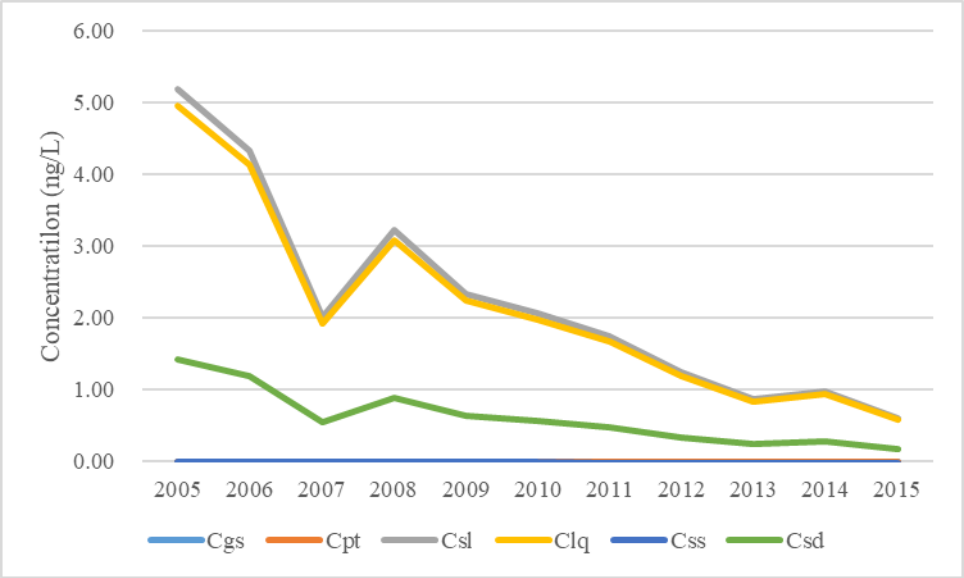

Figure 35. Concentration of Albon in each media.

Considering the volume of the environment media, the annual average concentration of chemicals was shown in Figure 34 – 35. The average number of SMX concentration was around 18 ng/L in water, 11 ng/L in soil, 5 ng/L in sediment. And the average number of Albon was around 2 ng/L in water, 2 ng/L in soil, 0.6 ng/L in sediment. Both SMX and Albon showed a quite low-level environmental concentration. According to the

calculation, there was no accumulation during the year. The chemical soon came to the equilibrium after discharged in to the environment.

5.4.2 Spatial distribution

The spatial distribution of annual average concentration in soil media (Figure 36 – 37) shows that the sulfa-drug was mainly concentrated in same place where the emission was concentrated as well, with the maximum SMX concentration of 600 ng/L and the maximum Albon concentration of 150 ng/L. Meanwhile, the distribution of annual average concentration in water media is different from that in soil. Although the emission was all assumed to be discharged into the soil, because of the fluxes between water and soil such as rainfall land loss, some chemicals move to the water media. Some mesh with large rivers had a lower level of the sulfa-drug concentration because the water flow was large, bringing a lot of clean water which dilute the chemicals. The annual concentration of Albon was decreasing while SMX was basically the same both in soil and water media that were consistent with the results of emissions estimation.

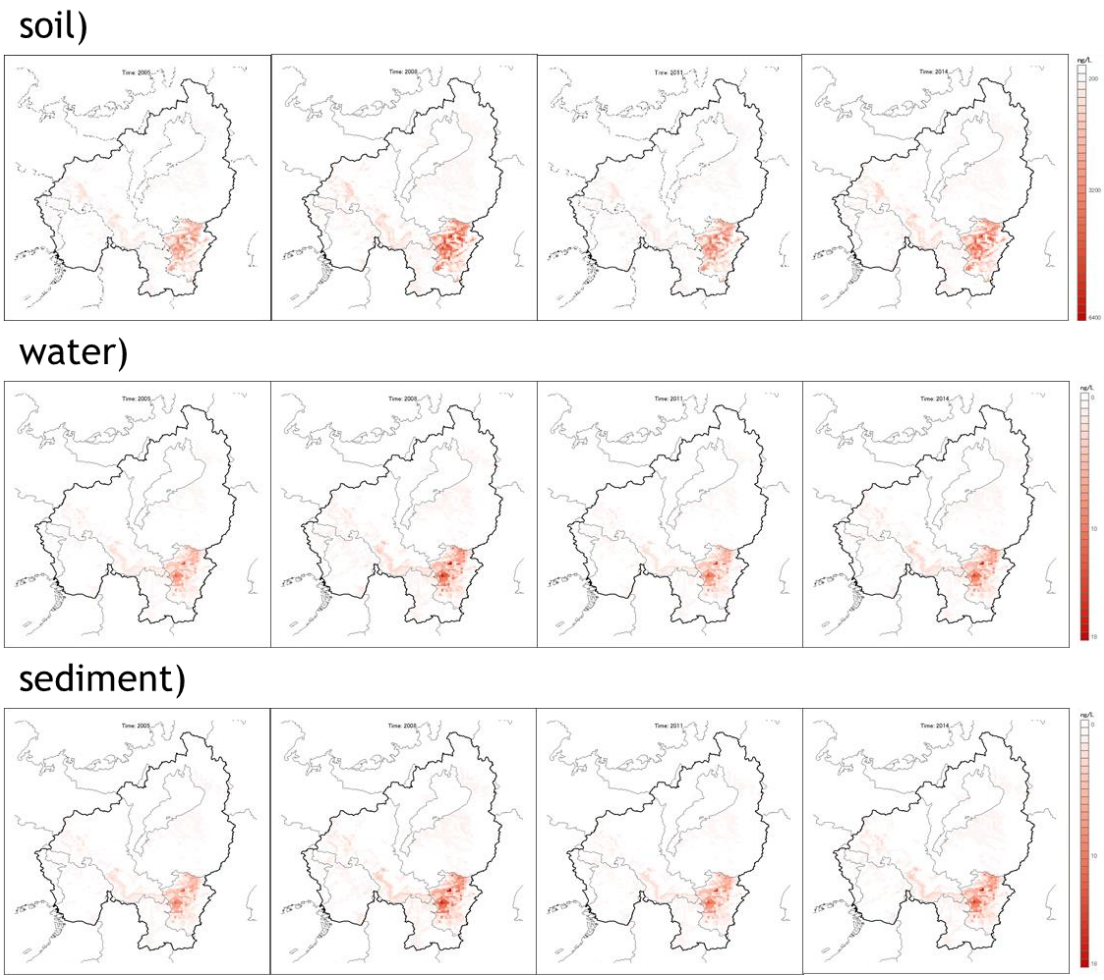

Figure 36. Distribution of SMX in soil, water and sediment.

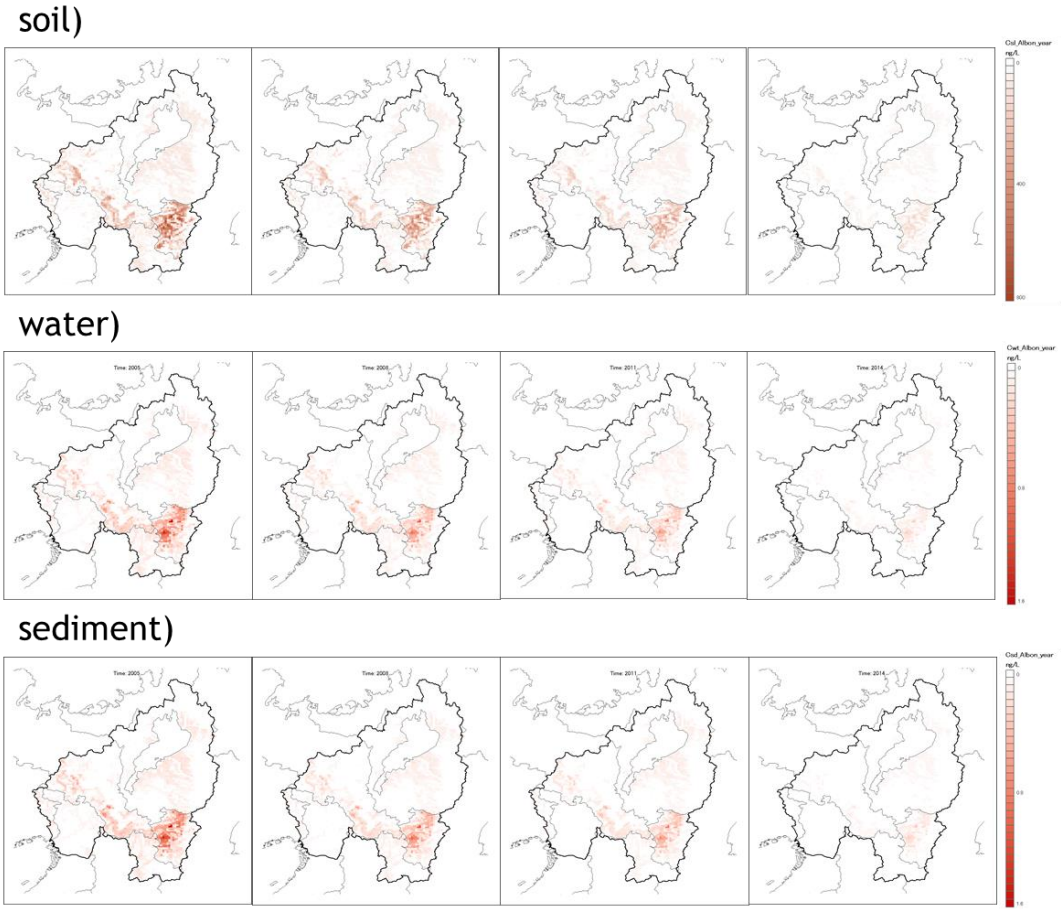

Figure 37. Distribution of Albon in soil, water and sediment.

5.4.3 Comparison

Compare to the result of one-box model, there were more residual in the environment. The distributional type model shows more concentration in the environmental media. In soil media, the concentration of SMX and Albon was around 200 ng/L and 20 ng/L. But looking the distribution or proportion of each media, the chemical was mainly absorbed in the soil media (almost 100%), and only a few were in water media or in the lake. However, Albon has been detected in the water system inside the Lake Biwa and Yodo River Basin in 2006. The observation concentration was around 15 ng/L, which was higher than the simulation result.

5.5 Conclusion

Sulfa drugs, as one of the antibiotics, are wildly used in the world, the potential environmental risk to both human health and ecological system attracted a lot of attentions. In order to estimate risk assessment, it is necessary to make accurate estimation of sulfa drugs concentration in the environment.

This part of study constructed a fate prediction model to express the dynamics of sulfa drugs in the atmosphere, water, soil and sediments, and analyze the behavior between environmental media. In this application of the distributional multimedia model, both distributional type model and the original one box type model were utilized to analysis the environmental behavior of sulfa-drugs. The spatial and temporal variation of 2 sulfa drugs (SMX and Albon) concentration in the Lake Biwa-Yodo River Basin was estimated for recent years.

However, fate prediction models targeting veterinary medicine substances are very limited compared to those targeting high toxic heavy metals. Due to the lack of observational data for further comparison, the model still has errors in the prediction of organic pollutants. The observation was higher than the prediction, which implied that higher concentrations of the sulfa drugs may exist in reality. Although acute toxicity has not been demonstrated at this time, it warrants further attention and deeper study.

Limitations of the current work that need to be solved include

1. Lacking of future observation data in the study area to evaluating the model; the observation data was based on the sampling in year 2006, which only reflected the local real-time situation at that time. The single point could not reflect the situation of the whole region well leading to error of the whole time period simulation.

2. Improving the accuracy of fundamental data which were used during the simulation; the static data including meteorological and hydrology data were mostly based on the

year 2009 which might be out of time.

3. Reducing the error caused by assumptions and simplifications in methodology. The method that used to estimate the emission was simplified as the proportion of livestock excrement. Both the 6 prefectures usage of the whole country and the spatial distribution was based on the farmland proportion. It is necessary to make further considerations, such as the administration period, species difference, mechanisms of drug metabolism, and even the location of the livestock farm. These conditions may cause the underestimation. The above limitations require further studies in order to evaluate the potential risk of long-term exposure of such concentration level of these 2 sulfa drugs. The sulfa drug was a group of chemicals, the rest of them not mentioned in this study may be also toxic to the human healthy and ecosystem after discharged into the environment without treatment. People need to be alert to the adverse environmental impacts of veterinary medicine discharged into the environment.

6 Conclusion and recommendation

6.1 Conclusion

In this study, distributional type multimedia model was developed based on a one-box type model. The model was utilized to 3 type different environmental chemicals in the Lake Biwa-Yodo River Basin, Japan. The study area was divided into tiny meshes, and each was divided into four environmental media: atmosphere, soil, water body, and sediment. According to the behavior of different pollutants in environmental media, we modified the core of the model and constructed the corresponding equations respectively. At the same time, we estimated the emissions for the three type pollutants. The concentration of pollutants in the target area was calculated over a long period of time by substituting into the model using meteorological and hydrological land data that exist in reality. For Pb, the model calculated the concentration 60 years from 1957 to 2016. The amount of Pb distributed into each mesh inside the basin. The validity of the distributional model was evaluated by comparing it with measured Pb concentrations. By compare to the observation, the model could predict Pb well.

Different to Pb, we consider material transformations of Hg in our model while introducing possible stars for external contamination. The calculated Hg concentrations no longer raised significantly and were becoming constant due to Japan successfully controlled the national usage of Hg. Through more specific comparisons down to individual observation stations, we found that the model can predict behavior of Hg in our target area. Both environmental concentrations and the distribution had been validated. Having successfully predicted the environmental fate of metals, this study turned its attention to organic refractory pollutants. This study attempts to push the model into a

wider range of predictions. We successfully modified the parameters of the model and tried to predict the concentration distribution of 2 drugs. We calculated the possible spatial distribution of the drug. However, the measured values were higher than the model predictions and our model still has very many shortcomings in the prediction of pollutants in this project, which needs to be improved urgently in the subsequent research work.

6.2 Recommendation

In this study, the model exists with a large number of assumptions and simplifications that facilitate the calculations. These assumptions and simplifications have somewhat led to a gap between our calculations and reality. In terms of the input data, although official and credible data were used as far as possible, some estimation was made in details such as the emission and location of pollutants. These estimations are subject to a high degree of uncertainty and may be diametrically opposed to reality. There are a large number of unknown influences. At the same time, we have reused some of the data in our calculations using computers. For example, we let the weather conditions repeat over and over again, however in reality there are uncontrollable factors such as typhoons and floods. These extreme conditions can cause a lot of deflection of pollutants. The calculation of this model requires a large amount of data, which is still time-consuming despite the assistance of computers.

All of these, as mentioned above, are problems exposed by this study. More work is needed if the present model is to be applied to other pollutants, or to other regions. This paper suggests that future research could focus on these areas.

References

Abdel Gawad, S.S., 2018. Concentrations of heavy metals in water, sediment and mollusk gastropod, Lanistes carinatus from Lake Manzala, Egypt. The Egyptian Journal of Aquatic Research 44, 77-82.

Abou-Elwafa, S.F., Amin, A.E.-E.A.Z., Shehzad, T., 2019. Genetic mapping and transcriptional profiling of phytoremediation and heavy metals responsive genes in sorghum. Ecotoxicology and Environmental Safety 173, 366-372.

Akiko Kida, 2012. Japan and the World Mercury Use and Emissions. Public Seminar on Mercury Convention, Makuhari, Chiba City, Japan.

Akitomo, K., Tanaka, K., Kumagai, M., Jiao, C., 2009. Annual cycle of circulations in Lake Biwa, part 1: model validation. Limnology 10, 105-118.

Alghamdi, B.A., El Mannoubi, I., Zabin, S.A., 2019. Heavy metals' contamination in sediments of Wadi Al-Aqiq water reservoir dam at Al-Baha region, KSA: Their identification and assessment. Human and Ecological Risk Assessment: An International Journal 25, 793-818.

Ali, H., Khan, E., 2018. Assessment of potentially toxic heavy metals and health risk in water, sediments, and different fish species of River Kabul, Pakistan. Human and Ecological Risk Assessment: An International Journal 24, 2101-2118.

Angle, C.R., Marcus, A., Cheng, I.H., McIntire, M.S., 1984. Omaha childhood blood lead and environmental lead: A linear total exposure model. Environmental Research 35, 160-170.

Boxall, A.B., Rudd, M.A., Brooks, B.W., Caldwell, D.J., Choi, K., Hickmann, S., Innes, E., Ostapyk, K., Staveley, J.P., Verslycke, T., Ankley, G.T., Beazley, K.F., Belanger, S.E., Berninger, J.P., Carriquiriborde, P., Coors, A., Deleo, P.C., Dyer, S.D., Ericson, J.F., Gagné, F., Giesy, J.P., Gouin, T., Hallstrom, L., Karlsson, M.V., Larsson, D.G., Lazorchak, J.M., Mastrocco, F., McLaughlin, A., McMaster, M.E., Meyerhoff, R.D., Moore, R., Parrott, J.L., Snape, J.R., Murray-Smith, R., Servos, M.R., Sibley, P.K., Straub, J.O., Szabo, N.D., Topp, E., Tetreault, G.R., Trudeau, V.L., Van Der Kraak, G., 2012. Pharmaceuticals and personal care products in the environment: what are the big questions? Environ Health Perspect 120, 1221-1229.

Brandes, L., Den Hollander, H., 1996. SimpleBox 2.0: a nested multimedia fate model for evaluating the environmental fate of chemicals.

Buhari, O., Atanda, A., Alzharani, T., Faillace, R., 2019. EXPOSURE TO HEAVY METALS MAY INCREASE CARDIOVASCULAR RISK BY ELEVATION OF SERUM LIPID LEVELS AND HEMOGLOBIN A1C: A NATIONAL HEALTH AND NUTRITION EXAMINATION SURVEY BASED STUDY. Journal of the American College of Cardiology 73, 1882.

Center for Global Environmental Research, East Asian Air Pollutant Emissions Grid Database.

Chai, M., Li, R., Ding, H., Zan, Q., 2019. Occurrence and contamination of heavy metals in urban

mangroves: A case study in Shenzhen, China. Chemosphere 219, 165-173.
Chowdhury, S., Mazumder, M.A.J., Al-Attas, O., Husain, T., 2016. Heavy metals in drinking water: Occurrences, implications, and future needs in developing countries. Science of The Total Environment 569-570, 476-488.
Csiszar, S.A., Diamond, M.L., Thibodeaux, L.J., 2012. Modeling urban films using a dynamic multimedia fugacity model. Chemosphere 87, 1024-1031.
Den Hollander, H., Van de Meent, D., 2004. Model parameters and equations used in Simplebox 3.0. Bilthoven, RIVM, report.
Diamond, M.L., Priemer, D.A., Law, N.L., 2001. Developing a multimedia model of chemical dynamics in an urban area. Chemosphere 44, 1655-1667.
Douay, F., Pelfrêne, A., Planque, J., Fourrier, H., Richard, A., Roussel, H., Girondelot, B., 2013. Assessment of potential health risk for inhabitants living near a former lead smelter. Part 1: metal concentrations in soils, agricultural crops, and homegrown vegetables. Environmental Monitoring and Assessment 185, 3665-3680.
Du, W., Liu, M., Li, Y., Zhu, J., Wei, X., Yang, J., Huang, Y., Zhao, D., Gao, D., Qadeer, A., 2020. Cross-interface transfer of polycyclic aromatic hydrocarbons (PAHs) in a shallow urban lake in Shanghai, China based on the fugacity model. Science of The Total Environment 736, 139369.
Edwards, F.G., Egemen, E., Brennan, R., Nirmalakhandan, N., 1999. Ranking of toxics release inventory chemicals using a Level III fugacity model and toxicity. Water Science and Technology 39, 83-90.
Esdaile, L.J., Chalker, J.M., 2018. The mercury problem in artisanal and small‐scale gold mining. Chemistry–A European Journal 24, 6905-6916.
Feenstra, S., Mackay, D.M., Cherry, J.A., 1991. A Method for Assessing Residual NAPL Based on Organic Chemical Concentrations in Soil Samples. Groundwater Monitoring & Remediation 11, 128-136.
FUKUI, T., Kuniyori, K., Baba, T., Kannari, Y., 2014. Annual update of the air pollutant emission inventory EAGrid2000-Japan. Journal of the Atmospheric Environment Society 49, 117-125.
Gholizadeh, M., Patimar, R., 2018. Ecological risk assessment of heavy metals in surface sediments from the Gorgan Bay, Caspian Sea. Marine Pollution Bulletin 137, 662-667.
Gu, Y.-G., Lin, Q., Huang, H.-H., Wang, L.-g., Ning, J.-J., Du, F.-Y., 2017. Heavy metals in fish tissues/stomach contents in four marine wild commercially valuable fish species from the western continental shelf of South China Sea. Marine Pollution Bulletin 114, 1125-1129.
Hernberg, S., 2000. Lead poisoning in a historical perspective. American journal of industrial medicine 38, 244-254.
Hu, H., Lin, H., Zheng, W., Tomanicek, S.J., Johs, A., Feng, X., Elias, D.A., Liang, L., Gu, B., 2013. Oxidation and methylation of dissolved elemental mercury by anaerobic bacteria. Nature

Geoscience 6, 751-754.
Jaffe, D., Strode, S., 2008. Sources, fate and transport of atmospheric mercury from Asia. Environmental Chemistry - ENVIRON CHEM 5.
Japan Meteorological Agency, 2011. Heavy metals (past diagnosis).
Japan Meteorological Business Support Center, Meso Numerical Prediction Model GPV (MSM).
Japan Paint Manufacturers Association, Monthly Report of Chemical Industry Statistics, Ministry of Economy, Trade and Industry.
Kampa, M., Castanas, E., 2008. Human health effects of air pollution. Environmental Pollution 151, 362-367.
Karar, S., Hazra, S., Das, S., 2019. Assessment of the heavy metal accumulation in the Blue Swimmer Crab (Portunus pelagicus), northern Bay of Bengal: Role of salinity. Marine Pollution Bulletin 143, 101-108.
Kawashima, M.O.U., Suita (Japan)), Tobe, T., Kaga, A., Kondo, A., Inoue, Y., Tatsuwaki, K., 2007. Screening level environmental risk evaluation of PRTR chemicals in Lake Biwa and the Yodogawa Basin Area [Japan]. v. 20.
Kojiri, T., Hamaguchi, T., Ode, M., 2008. Assessment of global warming impacts on water resources and ecology of a river basin in Japan. J HYDRO-ENVIRON RES 1, 164-175.
Kondo, A., Yamamoto, M., Inoue, Y., Ariyadasa, B.H., 2013. Evaluation of lead concentration by one-box type multimedia model in Lake Biwa-Yodo River basin of Japan. Chemosphere 92, 497-503.
Krasnići, N., Dragun, Z., Erk, M., Raspor, B., 2013. Distribution of selected essential (Co, Cu, Fe, Mn, Mo, Se, and Zn) and nonessential (Cd, Pb) trace elements among protein fractions from hepatic cytosol of European chub (Squalius cephalus L.). Environmental Science and Pollution Research 20, 2340-2351.
Lake Biwa-Yodo River Water Quality Preservation Organization, Current status of the water environment in the Lake Biwa and Yodo River basins.
Lanphear, B.P., Matte, T.D., Rogers, J., Clickner, R.P., Dietz, B., Bornschein, R.L., Succop, P., Mahaffey, K.R., Dixon, S., Galke, W., Rabinowitz, M., Farfel, M., Rohde, C., Schwartz, J., Ashley, P., Jacobs, D.E., 1998. The Contribution of Lead-Contaminated House Dust and Residential Soil to Children's Blood Lead Levels: A Pooled Analysis of 12 Epidemiologic Studies. Environmental Research 79, 51-68.
Lentini, P., Poghosyan, L., Ronco, C., 2009. CHAPTER 313 - Lead and Heavy Metals and the Kidney. in: Ronco, C., Bellomo, R., Kellum, J.A. (Eds.). Critical Care Nephrology (Second Edition). W.B. Saunders, Philadelphia, pp. 1705-1711.
Li, G., Zhang, Z., Sun, H., Chen, J., An, T., Li, B., 2013. Pollution profiles, health risk of VOCs and biohazards emitted from municipal solid waste transfer station and elimination by an

integrated biological-photocatalytic flow system: A pilot-scale investigation. Journal of Hazardous Materials 250-251, 147-154.
Li, H., Xu, L., Feng, N., Lu, A., Chen, W., Wang, Y., 2021. Occurrence, risk assessment, and source of heavy metals in Liaohe River Protected Area from the watershed of Bohai Sea, China. Marine Pollution Bulletin 169, 112489.
Liang, Q., Xue, Z.-J., Wang, F., Sun, Z.-M., Yang, Z.-X., Liu, S.-Q., 2015. Contamination and health risks from heavy metals in cultivated soil in Zhangjiakou City of Hebei Province, China. Environmental Monitoring and Assessment 187, 754.
Liu, H.H., Cohen, Y., 2014. Multimedia Environmental Distribution of Engineered Nanomaterials. Environ. Sci. Technol. 48, 3281-3292.
Liu, J., Shi, J.-Z., Yu, L.-M., Goyer, R.A., Waalkes, M.P., 2008. Mercury in Traditional Medicines: Is Cinnabar Toxicologically Similar to Common Mercurials? Experimental Biology and Medicine 233, 810-817.
Liu, J., Wang, Y., Liu, X., Xu, J., 2021. Occurrence and health risks of heavy metals in plastic-shed soils and vegetables across China. Agriculture, Ecosystems & Environment 321, 107632.
Liu, M., Yin, H., Wu, Q., 2019a. Occurrence and health risk assessment of pharmaceutical and personal care products (PPCPs) in tap water of Shanghai. Ecotoxicology and Environmental Safety 183, 109497.
Liu, X., Lu, S., Guo, W., Xi, B., Wang, W., 2018. Antibiotics in the aquatic environments: A review of lakes, China. Science of The Total Environment 627, 1195-1208.
Liu, Y., Zhang, S., Li, C., Shi, X., Zhao, S., Sun, B., Zhu, Y., 2019b. A modified QWASI model for fate and transport modeling of Zn and Pb in a shallow lake during the ice-free period. Science of The Total Environment 657, 577-584.
Ma, L., Liu, Y., Yang, Q., Jiang, L., Li, G., 2022. Occurrence and distribution of Pharmaceuticals and Personal Care Products (PPCPs) in wastewater related riverbank groundwater. Science of The Total Environment 821, 153372.
Mackay, D., Diamond, M., 1989. Application of the QWASI (Quantitative Water Air Sediment Interaction) fugacity model to the dynamics of organic and inorganic chemicals in lakes. Chemosphere 18, 1343-1365.
Mackay, D., Paterson, S., Cheung, B., Neely, W.B., 1985. Evaluating the environmental behavior of chemicals with a level III fugacity model. Chemosphere 14, 335-374.
Mackay, D., Paterson, S., Joy, M., 1983. A quantitative water, air, sediment interaction (QWASI) fugacity model for describing the fate of chemicals in rivers. Chemosphere 12, 1193-1208.
Meent, D., 1993. SimpleBox: a generic multimedia fate evaluation model. National Institute of Public Health and Environmental Protection.
Meesters, J.A.J., Koelmans, A.A., Quik, J.T.K., Hendriks, A.J., van de Meent, D., 2014. Multimedia

Modeling of Engineered Nanoparticles with SimpleBox4nano: Model Definition and Evaluation. Environ. Sci. Technol. 48, 5726-5736.
Ministry of Agriculture Forestry and Fisheries, Annual Report of Sales Amount and Sales Volume of Veterinary drugs, Quasi-drugs and Medical Devices.
Ministry of Economy Trade and Industry, 2001. The PRTR System.
Ministry of Economy Trade and Industry, 2022. Industrial Statistics Survey.
Ministry of Land Infrastructure Transport and Tourism, Annual Report of Road Statistics 2011.
Ministry of Land Infrastructure Transport and Tourism, 2022. National Land Numerical Information Download Service.
Ministry of the Environment, 2020. Yearly measurement results of atmospheric mercury concentration at Cape Hedo (annual average).
Na, G., Ye, J., Li, R., Gao, H., Jin, S., Gao, Y., Hou, C., Huang, J., 2021. Fate of polycyclic aromatic hydrocarbons in the Pacific sector of the Arctic Ocean based on a level III fugacity environmental multimedia model. Marine Pollution Bulletin 166, 112195.
Nakagawa, R., Kato, T., Zhu, Z.m., 1991. Dynamics of Pesticide Mercury Residues in Paddy Soil. Journal of the Chemical Society of Japan 5, 7.
Norihiro Kobayashi, NAITO Wataru, 2006. Lead. Risk Assessment Documents. MARUZEN GROUP.
Orescanin, V., Katunar, A., Kutle, A., Valkovic, V., 2003. Heavy Metals in Soil, Grape, and Wine. Journal of Trace and Microprobe Techniques 21, 171-180.
Organization;, W.H., Mercury and health.
Osaka Prefecture Government, 2022. Hazardous Air Pollutant Monitoring Survey Results.
Peng, C., Zhang, K., Wang, M., Wan, X., Chen, W., 2022. Estimation of the accumulation rates and health risks of heavy metals in residential soils of three metropolitan cities in China. Journal of Environmental Sciences 115, 149-161.
Prabagar, S., Dharmadasa, R.M., Lintha, A., Thuraisingam, S., Prabagar, J., 2021. Accumulation of heavy metals in grape fruit, leaves, soil and water: A study of influential factors and evaluating ecological risks in Jaffna, Sri Lanka. Environmental and Sustainability Indicators 12, 100147.
Rabinowitz, M.B., Needleman, H.L., 1982. Temporal Trends in the Lead Concentrations of Umbilical Cord Blood. Science 216, 1429-1431.
Raknuzzaman, M., Ahmed, M.K., Islam, M.S., Habibullah-Al-Mamun, M., Tokumura, M., Sekine, M., Masunaga, S., 2016. Trace metal contamination in commercial fish and crustaceans collected from coastal area of Bangladesh and health risk assessment. Environmental Science and Pollution Research 23, 17298-17310.
Ramírez, N., Cuadras, A., Rovira, E., Borrull, F., Marcé, R.M., 2012. Chronic risk assessment of exposure to volatile organic compounds in the atmosphere near the largest Mediterranean

industrial site. Environment International 39, 200-209.
Roper, W.L., Houk, V., Falk, H., Binder, S., 1991. Preventing lead poisoning in young children: A statement by the Centers for Disease Control, October 1991. Centers for Disease Control, Atlanta, GA (United States).
Schipper, L.A., Sparling, G.P., Fisk, L.M., Dodd, M.B., Power, I.L., Littler, R.A., 2011. Rates of accumulation of cadmium and uranium in a New Zealand hill farm soil as a result of long-term use of phosphate fertilizer. Agriculture, Ecosystems & Environment 144, 95-101.
Shiga Prefectural Government, Overview of Lake Biwa.
Shrestha, K.L., Kondo, A., 2015. Assessment of the Water Resource of the Yodo River Basin in Japan Using a Distributed Hydrological Model Coupled with WRF Model. in: Ramkumar, M., Kumaraswamy, K., Mohanraj, R. (Eds.). Environ. Manag. River Basin Ecosyst. Springer International Publishing, Cham, pp. 137-160.
Singh, V., Suthar, S., 2021. Occurrence, seasonal variation, mass loading and fate of pharmaceuticals and personal care products (PPCPs) in sewage treatment plants in cities of upper Ganges bank, India. Journal of Water Process Engineering 44, 102399.
Sun, Q., Li, Y., Li, M., Ashfaq, M., Lv, M., Wang, H., Hu, A., Yu, C.-P., 2016. PPCPs in Jiulong River estuary (China): Spatiotemporal distributions, fate, and their use as chemical markers of wastewater. Chemosphere 150, 596-604.
Tamtam, F., Mercier, F., Le Bot, B., Eurin, J., Tuc Dinh, Q., Clément, M., Chevreuil, M., 2008. Occurrence and fate of antibiotics in the Seine River in various hydrological conditions. Sci Total Environ 393, 84-95.
Tamura, I., Yasuda, Y., Kagota, K.I., Yoneda, S., Nakada, N., Kumar, V., Kameda, Y., Kimura, K., Tatarazako, N., Yamamoto, H., 2017. Contribution of pharmaceuticals and personal care products (PPCPs) to whole toxicity of water samples collected in effluent-dominated urban streams. Ecotoxicol Environ Saf 144, 338-350.
Wang, Q., Fan, Z., Qiu, L., Liu, X., Yin, Y., Ibrahim. Jamus, I.m., Song, C., Chen, J., 2021. Occurrence and health risk assessment of residual heavy metals in the Chinese mitten crab (Eriocheir sinensis). Journal of Food Composition and Analysis 97, 103787.
Wuana, R., Okieimen, F., 2011. Heavy Metals in Contaminated Soils: A Review of Sources, Chemistry, Risks and Best Available Strategies for Remediation. ISRN Ecology 2011.
Xu, M., Huang, H., Li, N., Li, F., Wang, D., Luo, Q., 2019. Occurrence and ecological risk of pharmaceuticals and personal care products (PPCPs) and pesticides in typical surface watersheds, China. Ecotoxicology and Environmental Safety 175, 289-298.
Yang, Y., Xu, C., Cao, X., Lin, H., Wang, J., 2017. Antibiotic resistance genes in surface water of eutrophic urban lakes are related to heavy metals, antibiotics, lake morphology and anthropic impact. Ecotoxicology 26, 831-840.

Yodogawa River Office, Overview and various aspects of the Yodo River basin.
Yu, B., Wang, X., Dong, K.F., Xiao, G., Ma, D., 2020. Heavy metal concentrations in aquatic organisms (fishes, shrimp and crabs) and health risk assessment in China. Marine Pollution Bulletin 159, 111505.
Zhang, L., Wang, S., Wang, L., Wu, Y., Duan, L., Wu, Q., Wang, F., Yang, M., Yang, H., Hao, J., Liu, X., 2015. Updated Emission Inventories for Speciated Atmospheric Mercury from Anthropogenic Sources in China. Environmental Science & Technology 49, 3185-3194.